Response to interactive comment on "At which time scale does the complementary principle perform best on evaporation estimation?" by Liming Wang et al.

(Reviewers comments in Italic and responses in upright Roman)

Editor

Your paper has been reviewed by 3 reviewers. You have received 1 very critical review, and 2 reviews that consider proceeding with revisions. You've provided detailed replies to the concern as raised by the reviewers. After carefully reading the review reports and your rebuttal, I suggest to proceed with a major revision in which you include the suggested revisions. The revised manuscript shall be resend to the critical referee for a review of the revised manuscript.

Thank you for providing the opportunity to submit the revision of this work. We sincerely appreciate the comments of both editor and the reviewers. The detailed constructive comments are critically important for us to improve the manuscript. In response to these comments, we have performed additional analyses and substantially improved the quality of the manuscript. We hope that the editor and reviewers will be favorably impressed by the revised version. The point-by-point responses were provided as follows.

Anonymous Referee #1

-The MS is carelessly written. It should be thoroughly rechecked for grammar, typos, language constructs.

Response: Thank you for the comments. We have gone through and revise the manuscript thoroughly and hired some language experts to help polish the manuscript again.

-For example, the AA method is mentioned several times before it is explained.

Response: Thank you for pointing out this problem. we had provided the full name for it when the first time it is mentioned (**Line 55-57, hereafter all lines numbers are based on the tracked version**). Also, we moved the explanation from the methodology part to the introduction part.

-Also, the first asymmetric AA method was of Kahler and Brutsaert (2006), and not by Brutsaert and Parlange (1998).

Response: According to our reading, Brutsaert and Parlange (1998) provided the following equation in their paper:

$$E = \left[(1 + b)E_0 - aE_{pa}\right]/b$$

where, E_0 has the same meaning of E_{po} in our manuscript (i.e., potential evaporation), and a is a pan coefficient, b is an asymmetric parameter. Our statement "the CR was extended to a linear function with an asymmetric parameter (Brutsaert and Parlange, 1998)" (**Line 57-58**) refers to this equation.

Kahler and Brutsaert (2006) summarized the previous work of Brutsaert and Stricker (1979), Brutsaert and Parlange (1998), and Brutsaert (2005) and gave the equation:

$$(1 + b)E_0 = C_p E_{pa} + bE$$

where, C_p is a constant parameter. We can see that this equation holds the same format with Brutsaert and Parlange (1998) after appropriate transformation (and replacing C_p with a). It may be the first time it was called "asymmetric AA". Thank you.

-Also, nobody reads the original work of Bouchet (1963), it seems, as it is in French. That may be the reason for frequent misquoting it. My understanding is that he never proposed a symmetrical CR. Even Brutsaert in his seminal book (1982) is controversial about this issue. The authors should clarify this issue though.

Response: Yes, the original work of Bouchet (1963) is French. In our institute of Tsinghua University, we have a PhD student coming from France, and he had translated this paper into English several years ago. We are pleased to provide the English version of Bouchet (1963) at the end of the response for the reference. After reading this paper, we suggest that the contribution of Bouchet (1963) should be respected.

Equation (5) and Figure 2 of Bouchet (1963) show a symmetrical complementary relationship:

$$ETP + ETR = 2ETP_0$$

where, ETR is the energy corresponding to the real evapotranspiration, ETP is corresponding to E_{pa}, and ETP_0 is corresponding to E_{po}.

In the book of Brutsaert (1982, p224-225), the above equation is cited as equation (10.35), and Brutsaert said that Bouchet (1963) arrived at the complementary relationship and admit Bouchet's approach contains worthwhile ideas and led to further developments. Brutsaert thought this method is not used widely because the assumption is strict and it did not provide exactly measures of E_{pa} and E_{po}. Thank you.

-I do not really see what we gain from this study. The high NSE value for the month comes about because its high variance between months and it is already being long enough to smooth things out.

Response: The aim of this study is to investigate at which time scale the complementary principle performs best on evaporation estimation. Based on this reviewer's comment, we understand that the reviewer gained that complementary functions perform best at the monthly scale. Actually, it's exactly what we want to convey to the audience. We did not find the evidence in previous studies or theoretical derivation which had already revealed this conclusion. Without these results, it is still uncertain how long is "enough to smooth things out". It could be 7 days, 30 days or 90 days. We agree with the reasons for the high NSE value at the monthly scale given by the reviewer, these reasons are also discussed in our manuscript (**Line 268- 272**). The "high variance" can be corresponding to our explanation about "variabilities of *x* and *y*" (**Line 272**), and the "smooth things out" can be corresponding to our explanation of RMSE. Thank you.

-I bet that between Mays, Junes, Julys, etc., the NSE value would not be better than for the seasons and years.

Response: In the current version, the study periods are from April to September for the Northern Hemisphere and from October to March for the Southern Hemisphere. We supposed that the reviewer mean that if the study periods are shortened (e.g, from May to July), the NSE values at the monthly scale will not be better than for the seasons and years. We have provided the results for May to July in **Table R1**. In this situation, the seasonal result is equal to the annual result and there is one seasonal result (May to July) each year. These results still support our conclusion. The NSE values at the monthly scale (NSE_H = 0.38 and NSE_B = 0.32) are higher than those at the seasonal/annual scale (NSE_B = −0.07 and NSE_B = −0.05). Thank you for providing an opportunity to test the uncertainty in the length of study periods.

Table R1. The evaluation merits (NSE, R^2 and, RMSE in W m^{-2}) of the two generalized complementary functions from May to July

	Month	Season/Year
NSE_H	0.38	−0.07
NSE_B	0.32	−0.05
$R^2{}_H$	0.63	0.56
$R^2{}_B$	0.63	0.56
$RMSE_H$	12.17	8.86
$RMSE_B$	21.51	8.81

-The low value for the annual time-scale is a bit worrisome as it means that these two chosen methods cannot replicate any long-term trends in ET rates to acceptable accuracy, which diminishes their potential values for long-term hydrological modeling.

Response: Yes, the complementary functions perform worse in estimating *E* at the annual scale. To the best of our knowledge, this point had not been thoroughly discussed previously. We did not recommend choosing the annual scale as the timestep to estimate *E* because of the low efficiency. However, we can still replicate the long-term trends in *E* rates by adopting the monthly timestep. Thank you.

Anonymous Referee #2

-Ln 9. Suggest change "Energy correction methods" to "energy balance closure methods"

Response: Thanks for your advice. The manuscript has been revised accordingly (**Line 9**).

-Ln 154-157, does this mean that the two model parameters (i.e. m and n) are determined from alpha and b only?

Response: Yes, it is. The variable $x_{0.5}$ in Eq. (4) is also determined by α and b ($x_{0.5} = \frac{0.5+b^{-1}}{\alpha(1+b^{-1})}$) only. Thus, all the parameters in Eq. (4) can be determined from α and b only. Thank you.

-Ln171-177, What is the justification for the treatment of parameter alpha?

Response: Thanks for your question. Typically, α has a default value of 1.26 (Priestley & Taylor, 1972). Since some studies showed that a constant α may cause irrational results and biases in estimating E, it is suggested to specify α for diverse scenarios (Hobbins, Ramírez, Brown, & Claessens, 2001; Ma et al., 2015; Sugita et al., 2001; Szilagyi, 2007). According to the complementary principle, in wet condition, E is close to E_{pen} (Penman evaporation) and the Priestley-Taylor's evaporation ($E_{PT} = \alpha\, E_{rad}$). Specifically, when E/E_{pen} is larger than a threshold (0.9 is commonly adopted), E_{PT} can be considered to approximately equal to the observed E, thus α can be calculated by E/E_{rad} (Kahler and Brutsaert, 2006; Ma et al., 2015). In this study, α was calculated by this method based on the mean value of E/E_{rad} in the wet condition ($E/E_{pen} > 0.9$). When all the E/E_{pen} values are less than 0.9, α is set as the default value of 1.26. The manuscript has been revised accordingly (**Lines 175-186**).

-Was the optimization done for each flux site at daily, weekly, monthly, and annual time scales respectively?

Response: Yes, the optimizations were done separately. Thank you.

-Why was equation (5) was tested instead of (6)? Brutsaert (2015) suggested that "it is preferable to use equation (6) and the c parameter should only be introduced to accommodate unusual situations."

Response: Thanks for your question. Brutsaert (2015) suggested that c should be 0 in usual situations, thus, the PGC function (Eq. (5)) becomes a concise cubic polynomial function including only two terms (Eq. (6)). Although the concise version of the PGC function has been frequently used recently (Brutsaert et al., 2017; Hu et al., 2018; Liu et al., 2016; Zhang et al., 2017), researchers still have different opinions on the true value of c. For example, Han and Tian (2018) found that the mean c value of the 20 sites of FLUXNET is −1 and Szilagyi et al. (2016) suggested that c is equal to 2 for 334 catchments in America. The results of Zhou et al. (2020) showed that the mean c value is 6.62 for 15 catchments on the Loess Plateau, China. Moreover, we had tested Eq. (6) in the analysis before, and the results showed that the performance of Eq. (6) is much worse than Eq. (5). We provided the results in **Table R2** and **Figure R1**. Since we have used the optimization algorithm to determine the parameter *b* in the SGC function, it is a fair manner to use the optimal *c* value instead of a constant value (*c* = 0) in the PGC function. The manuscript has been revised accordingly (**Lines 191-193**).

Table R2. The evaluation merits (NSE, R^2, and RMSE in W m^{-2}) based on Eq. (5) (optimal *c*) with the subscript B-5 and Eq. (6) (c = 0) with the subscript B-6.

	Day	Week	Month	Year
NSE_{B-5}	0.19	0.3	0.5	0.25
NSE_{B-6}	-0.47	-0.61	-0.69	-8.98
R^2_{B-5}	0.61	0.7	0.75	0.63
R^2_{B-6}	0.61	0.69	0.72	0.62
$RMSE_{B-5}$	26.83	19.17	13.7	6.96
$RMSE_{B-6}$	33.65	28.51	23.98	21.47

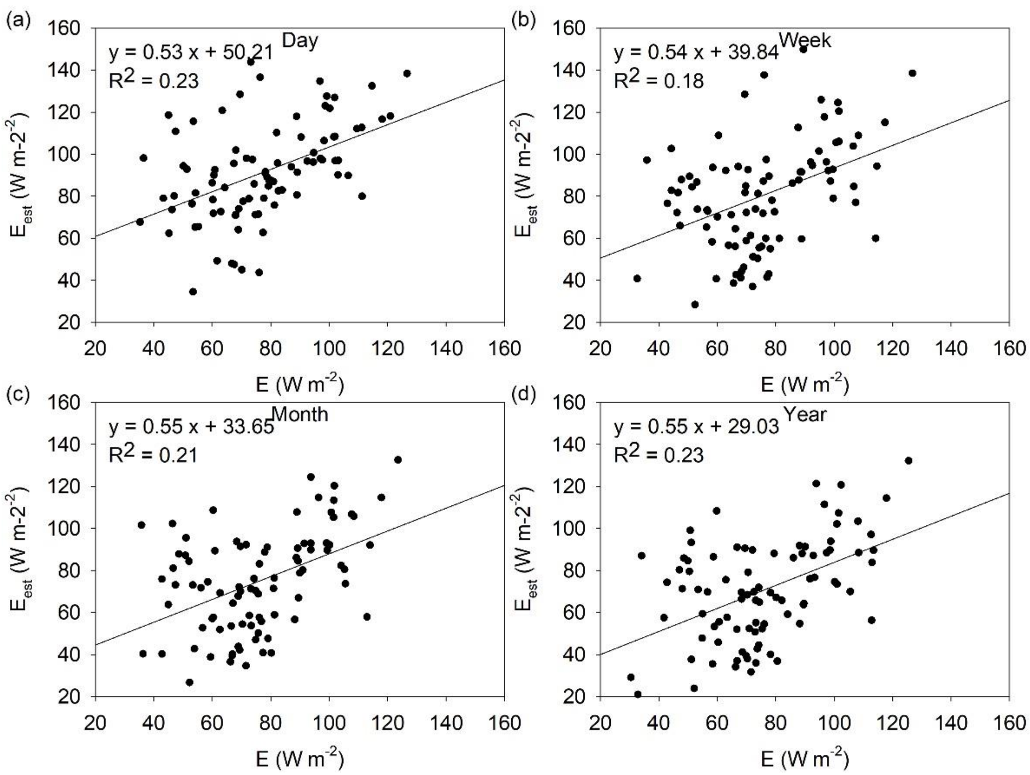

Figure R1. The estimated evaporation based on the polynomial function with c = 0 (equation (6)) vs the observed evaporation at daily scale (a), weekly scale (b), monthly scale (c), and yearly scale (d).

-Ln220-227, The results shown in Figure 1 do not indicate the model performance at daily, weekly, monthly, and annual time scales. If the authors want to know how the model performs

at these time scales, they need to show daily to annual results for each site and present a summary of the 88 flux sites.

Response: Thanks for your suggestion. Figure 1 just provides a general cognition of the performance. To accurately show the model efficiency at different time scales, we have provided the results at different timescales for each site in **Table S2** following the advice of the reviewer. A summary of these results have been added in the revision (**Lines 259-262**).

-Ln 241, Morton (1983) suggested that the complementary relationship should be applied at longer time scales (e.g. monthly), but it does not explain why the weekly or monthly results are better than the daily results.

Response: Yes, we agree with the reviewer. Morton (1983) just inferred that the complementary relationship should not be applied at short time scales because of the potential lag times associated with heat and water vapor change (p24 - p25 in Morton, 1983). However, it does not provide solid evidence or theoretical derivation to prove this inference. The statement has been revised (**Lines 272-277**). Thank you.

-Ln370, Figure 5 should be Figure 7. What is the significance of this relationship?

Response: Thanks for your careful review. The manuscript has been revised accordingly (**Lines 419-426**). The relationship provides the additional evidence besides Figure 2 that the two functions can substitute each other in a sense. In other words, the two functions with calibrated parameters substantially provide the similar descriptions of the distribution of results in the state space ($x = E_{rad}/E_{pen}$, $y = E/E_{pen}$). They can covert to each other in most situations since the two functions are roughly equivalent to the linear asymmetric function when x is neither excessively large nor excessively small.

-Ln 409 – 436, This section deals with the issue of the energy balance closure. To me, this is a separate question and I don't see the relevance to the performance of the complementary relationships.

Response: Thanks for your comment. This part has been deleted in the revision.

Anonymous Referee #3

Complementary evaporation relationships have been studied at multiple time scales, which time scale is the most suitable one? In this respect, the manuscript gave very meaningful results. It is recommended that the draft should be revised on the following questions before publication.

Thanks for your careful review and affirmation of this work. All the questions are very constructive and inspiring. The point-by-point responses were provided as follows.

-(1). Ln172-173, Ln458-459, "When all the E/E_{pen} values were less than 0.9, α was set as the default value of 1.26". This default value is problematic for the PGC model. The independent variable of PGC model is $E_{po}/E_{pa} = \alpha * E_{rad}/E_{pen}$, which is less than or equal to 1. When α =1.26, the range of E_{rad}/E_{pen} values is only 0-0.79. However, if α =1, the range of E_{rad}/E_{pen} values is 0-1. It could be imagined that the PGC cannot fit the data points with $0.79<E_{rad}/E_{pen}<1$ if the α =1.26, but there is no problem in the case of α =1.

Response: Thanks for your comment. Indeed, the PGC model does not work for the range of $0.79 < E_{rad}/E_{pen} < 1.0$ when α adopts its default value of 1.26 (Priestley & Taylor, 1972; Brutsaert & Stricker, 1979), which is a shortage of PGC. In our manuscript, α was calculated by the mean value of the ratio of E_{PT} to E_{rad} during the study period (similar treatment can be found in Kahler & Brutsaert, 2006). Such calculation is based on the physical definition of the Priestley-Taylor coefficient (i.e., α). Actually, the values of α for all sites besides those adopting α = 1.26 are greater than 1.0 in our study, which means the PGC model cannot work properly for the condition of $1/\alpha < E_{rad}/E_{pen} <1.0$.

In the submitted manuscript, the original results for $1/\alpha < E_{rad}/E_{pen} < 1$ calculated by the PGC function were kept. We have carried out an additional analysis that adopting $E = E_{pen}$ for $1/\alpha < E_{rad}/E_{pen} < 1$ in the PGC function, and the resultant NSE_B (0.19 vs 0.19) and $RMSE_B$ (26.83 W m^{-2} vs 26.68 W m^{-2}) presented very similar results. The manuscript has been revised to incorporate these discussions (**Lines 365-367**). Thank you.

-(2). Ln294-295, Ln336-337, Ln351-352,Ln466-467, The manuscript gave a conclusion that the parameter c of PGC model decreased with the increase of time scale. The parameter c was determined under the condition of a fixed α in this study, which needs to be specially explained. When the c is a fixed value, say 0, the α would change with the month (Liu et al.,2016).

Response: Thanks for your comment. To make the model parsimonious, it is a reasonable choice to give one value for the parameters α and c at each site for every different time scale. If the parameter was alterable, for example, it was monthly dependent, we will have to calibrate 12 parameters instead of one value for the whole study period. The purpose of this study is to find the most suitable timescale for the complementary functions, the variances of the key parameter within a timescale will introduce extra uncertainties. It is true that the accuracy will increase when an alterable parameter (that means higher number of parameters) is used, however, the probability of overfitting risk will increase at the same time. Besides, a general representation of the parameter is more helpful to detect its overall trend as the change of timescale than a group of parameters.

Moreover, we carried out an additional analysis that c is fixed to 0, and α is calibrated as α_e. We found that the two methods gave similar results (mean RMSE = 14.99 W m^{-2} for α_e vs 16.67 W m^{-2} for α) and the conclusion on the time scale issue is consistent by adopting either α or α_e in the analysis. Actually, the optimal α_e has a significantly negative linear relationship with the optimal c and the Pearson correlation coefficient is −0.8. It suggests that calibrating either of the two parameters (α_e and c) equivalent (Han et al., 2012). Thanks all the same, and the manuscript has been revised accordingly to incorporate these discussions (**Lines 195-204, 437-443**).

-(3). By using statistical indexes such as determination coefficient, the manuscript considered that the complementary relationship of a monthly scale was the best, but the other time scales were not poor and reached to a very significant level too. Does this mean that the complementary relationship on other time scales also exists significantly, not as Morton (1983) said, only at longer timescales?

Response: Thanks for your question. Yes, we found the two complementary functions perform reasonably well at shorter timescales (i.e., day and week) with pretty high R^2. Also, the estimations of site mean evaporation at shorter timescales are accurate (Figure 1 and Figure 3), especially for the SGC function. These indeed suggest the complementary relationship holds at relatively shorter time scales, or at least we can say that the generalized complementary functions have the ability to estimate the evaporation accurately even at the shorter timescales. The manuscript has been revised to incorporate these discussions (**Lines 373-377**). Thanks.

-(4). Ln23, "global water and energy cycle". Generally, water can have a cycle, but energy flows only.

Response: Thanks for your careful review. The statement has been revised as "global water cycle and energy balance" (**Line 25**).

References

Bouchet, R. J.: Evapotranspiration réelle et potentielle, signification climatique. IAHS Publ, 62, 134-142, 1963.

Brutsaert, W.: Evaporation into the atmosphere: theory, history and applications. Springer, New York, 1982

Brutsaert, W.,: Hydrology: An Introduction, 605 pp., Cambridge Univ. Press, New York. 2005

Brutsaert, W.: A generalized complementary principle with physical constraints for land-surface evaporation. Water Resour. Res., 51(10), 8087-8093, 2015. https://doi.org/10.1002/2015wr017720

Brutsaert, W., Li, W., Takahashi, A., Hiyama, T., Zhang, L., Liu, W. Z.: Nonlinear advection-aridity method for landscape evaporation and its application during the growing season in the southern Loess Plateau of the Yellow River basin. Water Resour. Res., 53(1), 270-282, 2017. https://doi.org/ 10.1002/2016wr019472

Brutsaert, W., Parlange, M. B.: Hydrologic cycle explains the evaporation paradox. Nature, 396(6706), 30-30, 1998. https://doi.org/ 10.1038/23845

Brutsaert, W., Stricker, H.: Advection-Aridity approach to estimate actual regional evapotranspiration. Water Resour. Res., 15(2), 443-450, 1979. https://doi.org/ 10.1029/WR015i002p00443

Han, S. J., Hu, H. P., Tian, F. Q.: A nonlinear function approach for the normalized complementary relationship evaporation model. Hydrol. Processes, 26(26), 3973-3981, 2012. https://doi.org/10.1002/hyp.8414

Han, S. J., Tian, F. Q.: Derivation of a sigmoid generalized complementary function for evaporation with physical constraints. Water Resour. Res., 54(7), 5050-5068, 2018. https://doi.org/10.1029/2017wr021755

Hobbins, M. T., Ramirez, J. A., Brown, T. C.: The complementary relationship in estimation of regional evapotranspiration: An enhanced Advection-Aridity model. Water Resour. Res., 37(5), 1389-1403, 2001. https://doi.org/10.1029/2000wr900359

Hu, Z. Y., Wang, G. X., Sun, X. Y., Zhu, M. Z., Song, C. L., Huang, K. W., Chen, X. P.: Spatial-temporal patterns of evapotranspiration along an elevation gradient on Mount Gongga, Southwest China. Water Resour. Res., 54(6), 4180-4192, 2018. https://doi.org/10.1029/2018wr022645

Kahler, D. M., Brutsaert, W.: Complementary relationship between daily evaporation in the environment and pan evaporation. Water Resour. Res, 42(5), 2006. https://doi.org/10.1029/2005WR004541

Liu, X. M., Liu, C. M., Brutsaert, W.: Regional evaporation estimates in the eastern monsoon region of China: Assessment of a nonlinear formulation of the complementary principle. Water Resour. Res., 52(12), 9511-9521, 2016. https://doi.org/10.1002/2016wr019340

Ma, N., Zhang, Y. S., Szilagyi, J., Guo, Y. H., Zhai, J. Q., Gao, H. F.: Evaluating the complementary relationship of evapotranspiration in the alpine steppe of the Tibetan Plateau. Water Resour. Res., 51(2), 1069-1083, 2015. https://doi.org/10.1002/2014wr015493

Morton, F. I.: Operational estimates of areal evapo-transpiration and their significance to the science and practice of hydrology. J. Hydrol., 66(1-4), 1-76, 1983. https://doi.org/10.1016/0022-1694(83)90177-4

Priestley, C. H. B., Taylor, R. J.: On the assessment of surface heat-flux and evaporation using large-scale parameters. Mon. Weather Rev., 100(2), 81-92, 1972. https://doi.org/10.1175/1520-0493(1972)100<0081:Otaosh>2.3.Co;2

Sugita, M., Usui, J., Tamagawa, I., & Kaihotsu, I.: Complementary relationship with a convective boundary layer model to estimate regional evaporation. Water Resour. Res., 37(2), 353-365, 2001.

https://doi.org/10.1029/2000wr900299
Szilagyi, J.: On the inherent asymmetric nature of the complementary relationship of evaporation. Geophys. Res. Lett., 34(2), L02405, 1-6, 2007. https://doi.org/10.1029/2006gl028708
Szilagyi, J., Crago, R., & Qualls, R. J.: Testing the generalized complementary relationship of evaporation with continental-scale long-term water-balance data. J. Hydrol., 540, 914-922, 2016. https://doi.org/10.1016/j.jhydrol.2016.07.001
Zhang, L., Cheng, L., Brutsaert, W.: Estimation of land surface evaporation using a generalized nonlinear complementary relationship. J. Geophys. Res. Atmos., 122(3), 1475-1487, 2017. https://doi.org/10.1002/2016jd025936
Zhou, H., Han, S., & Liu, W.: Evaluation of two generalized complementary functions for annual evaporation estimation on the Loess Plateau, China. J. Hydrol., 124980, 2020. https://doi.org/10.1016/j.jhydrol.2020.124980

Appendix:

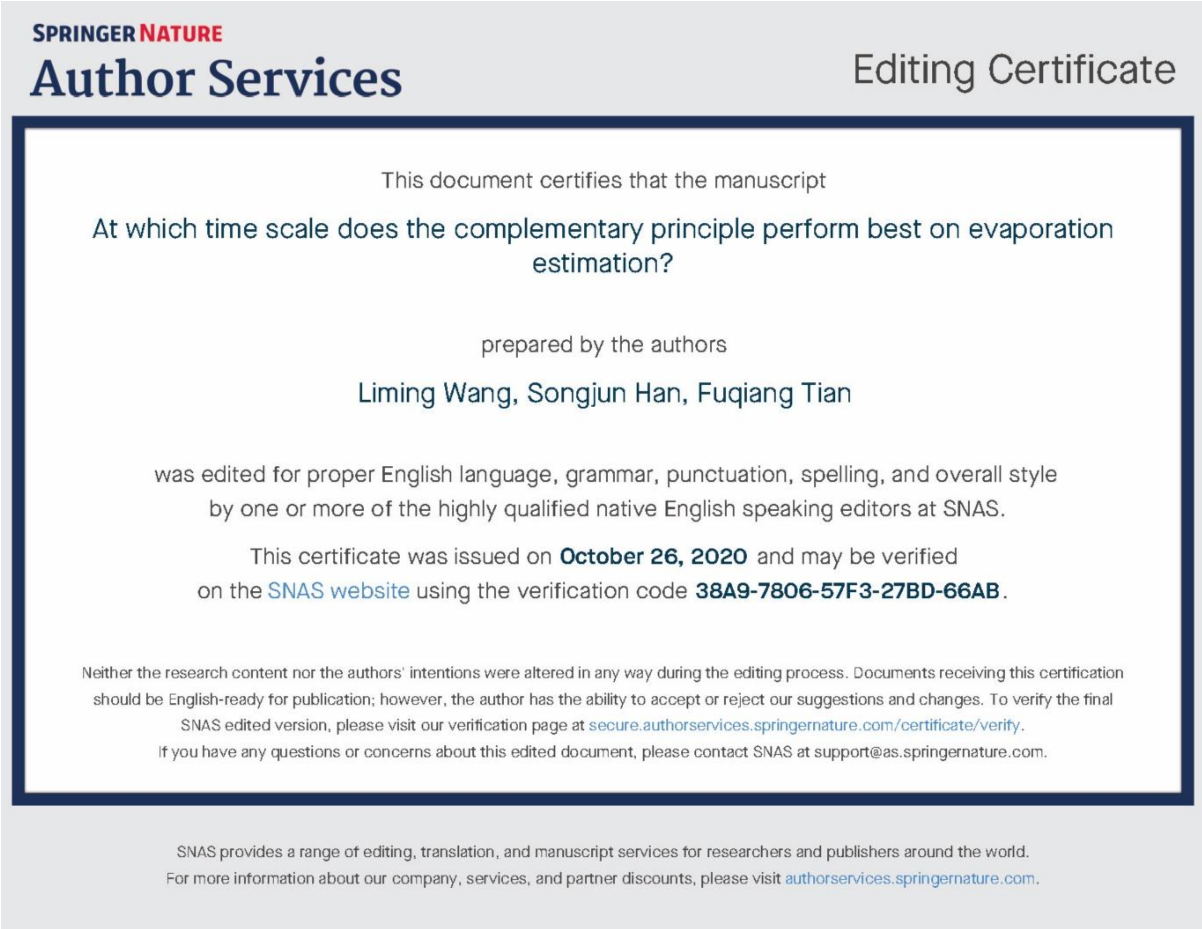

SPRINGER NATURE
Author Services

Editing Certificate

This document certifies that the manuscript

At which time scale does the complementary principle perform best on evaporation estimation?

prepared by the authors

Liming Wang, Songjun Han, Fuqiang Tian

was edited for proper English language, grammar, punctuation, spelling, and overall style by one or more of the highly qualified native English speaking editors at SNAS.

This certificate was issued on **October 26, 2020** and may be verified on the SNAS website using the verification code **38A9-7806-57F3-27BD-66AB**.

Neither the research content nor the authors' intentions were altered in any way during the editing process. Documents receiving this certification should be English-ready for publication; however, the author has the ability to accept or reject our suggestions and changes. To verify the final SNAS edited version, please visit our verification page at secure.authorservices.springernature.com/certificate/verify.
If you have any questions or concerns about this edited document, please contact SNAS at support@as.springernature.com.

SNAS provides a range of editing, translation, and manuscript services for researchers and publishers around the world.
For more information about our company, services, and partner discounts, please visit authorservices.springernature.com.

REAL EVAPOTRANSPIRATION AND POTENTIAL CLIMATIC SIGNIFICANCE

R . J . BOUCHET
Central station of bioclimatologie, Versailles
National institute of the Agronomic research (France)

The real evapotranspiration of an area represents the water really lost in the form of vapor, the potential evapotranspiration, the water likely to be lost under the same conditions when it is not limiting factor any more. The knowledge of these two data is obviously indispensable to study the circulation of water or to define the needs for the water of the cultures.

We propose to show the connections that exist not only between ETP and ETR, but also between these terms and the various elements of the energy report (the total radiation, the radiation of long wave, etc…), by using the method of the energy assessment. The simple relations that we will establish will permit to better define the climatic significance of ETR and ETP. It will then be possible to specify their respective variations when we will try to modify the climate in more or less vast zones, either by irrigating, or by changing the cover of the ground.

I -- STARTING ASSUMPTION -- SCALE OF THE ASSESSMENT

The study of the energy assessment supposes the preliminary definition of the system limits. To avoid taking into account the phenomena of accumulation and restitution of heating during the diurnal and night phases, the assessment will relate to one 24-hour period, the variations of temperature are then generally negligible.

The system includes the whole of the vegetable mass, a superficial section of ground, and a lower section of the atmosphere. Dimensions of these sections are just as the nycthemeral variations of temperature remain appreciable. The system exchange of heating with outside during this period takes place without the phenomena of radiation and evaporation, by conducting in deep layers of the ground (Qs) and by convecting (Qa) towards the high layers of atmosphere.

If this system itself is located in a zone that does not present the same climatic characteristics for various reasons, there will be the side exchanges of energy on the walls which has to be analyzed.

The side exchanges by conduction in the ground are negligible. It is not the same side exchange as in the atmosphere due to the movements of the standardized mass of air which we will indicate under the general name "of the oasis effects". Given the heterogeneity of a point to another of the type ground, the vegetable cover, the phenomena of evaporation, side movements of energy or "the oasis effect" are the rules under the natural conditions.

We can schematically represent the phenomenon of the oasis effect of the following manner (Fig. 1). If in a flat and homogeneous zone, an heterogeneity appears (the characteristics of the ground such as the thermal conductibility, the specific heating, the moisture or the nature of vegetable cover, the different ETR, etc…), it develops in the direction of the air circulation a disturbed zone where the medium factors find to be modified compared to the general climate because of heterogeneity. The oasis effect thus corresponds to an intrusion of the external system on the studied system, not only by its immediate edges but by the whole of the limit of the disturbed zone.

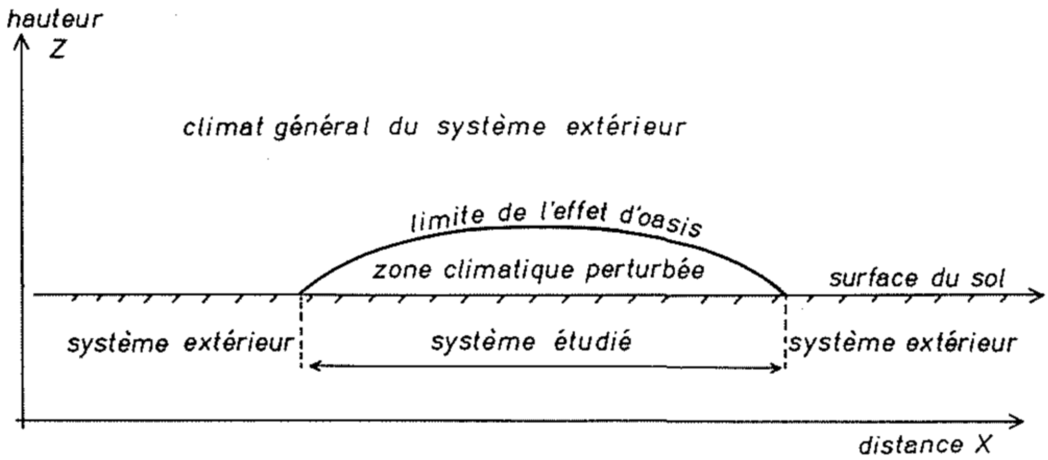

Fig. 1 -- Importance of the disturbed climatic zone according to the dimension of the heterogeneous system compared to the external system.
hauteur --- height;
climat général du système extérieur --- the general climate of external system
limite de l'effet d'oasis --- the limit of the effect of oasis
zone climatique perturbeé --- the perturbed climatic zone
surface du sol --- the ground surface
système extérieur --- the external system

The disturbance rises all the more in height since the heterogeneous zone is extended. It is always presented in the form of a "flat lens" for which the thickness is weak compared to horizontal dimensions. We can thus define, for each meteorological scale and each scale of heterogeneity, an oasis effect of corresponding scale (table 1) which gives the side exchange of energy Q_1 Q_2 Q_3 Q_4 Q_5. These are the exchanges that we will try to specify later on in the equation of the energy assessment and which we must take into account to define horizontal dimensions to give to the system.

As we propose to connect ETR to the different terms of the energy assessment, we must consider ETR as uniform on all the surfaces of the system. Thus it comes to determine from which minimum surface, the real evapotranspiration can affect the climatic factors that we use to define the climate, by acting on the energy assessment. It is only when we attain this minimum surface that we will be ensured to have an excellent connection between the climatic factors (θ_a, θ_r, wind, etc.) and ETR, since these factors will not only be considered any more as a more or less direct possible cause, but also as an effect. The minimum zone presenting the character of uniformity will have to thus be just as the disturbance reaches the level to which one refers to have the climatic data. Those are collected to 2 m above the ground with instruments having time-constants of the order of a minute. We will thus, a priori, have to consider only the thermal phenomena having a higher scale or equal to that of turbulence itself (> e_2).

The heating exchange of greater scale (e 3 4 5) are integrated in Qa term of the energy assessment. They thus contribute to define the climate. Thus, the "oasis effects" of great scale such as those existing between the maritime zones and the continents are found in the climatic data of the meteorological networks. In the same way, on the scale of the 1/2 day, the breezes of sea or ground can be treated as the oasis effects of higher scale or equal to e3.

The heating exchange related to the scales lower than e2 are from the concepts even of the negligible scale and can be regarded as the simple movements of standardization within the system which does not affect the climate just as we define it.

To respect the scale of turbulence, the zone considered for the energy assessment should thus take the character of uniformity on the distances of a few hundreds of meters, to see a few kilometers. The minimum extent on the surface is thus of the order from 10 to 100 ha.

TABLE 1

Scale (symbol in the text)	Scale of time	Scale of distance	Corresponding oasis effect (symbol in the text)
Molecular e1	10(-9) second		Q1
Turbulent e2	1s. to several minutes	A few hundreds of meters	Q2
Associated convection and movements e3	10 minutes to several hours	Several kilometers	Q3
Cyclonic e4	3 to 4 days	1000 to 2000 km	Q4
Planetary e5	10 to 30 days	5000 to 10,000 km	Q5

We define in Meteorology the scales of turbulence which permit to neglect the phenomena whose scale is small compared to the macroscopic movement considered.

On the whole of this surface, ETR will be uniform by hypothesis. If the real evapotranspiration around this system is different from that located inside, there will be the oasis effects; those will be all the more important scale because the zone considered will be large; within the framework of our definition, they will be lower or equal to turbulence. The potential evapotranspiration will be thus variable within the system according to the distance to these edges. The potential evapotranspiration then will be considered in the center of the device, where it is weakest or strongest. If the surface of the system were more important, ETP in the center would decrease or increase, but the climatic factors as they are generally considered, would then start to be affected, which would be against the starting hypothesis since we propose to define VETP of the initial climate and not Y ETP modified by the variations of evaporation.

In conclusion, ETP can be defined in the level of the meteorological shelter to 2 m only like the potential evapotranspiration in the center of a uniform zone at the view point of ground, vegetation or evaporation and at least few tens of hectares.

Thus, the reasoning which will follow will not be able to apply strictly to even the homogeneous zones which do not have the sufficient size and a fortiori, to the heterogeneous zones. We will thus encounter the great difficulties in defining ETR or ETP as the climatic factors in the zones of transition, because the oasis effects of scale lower than that used to define the climate, will modify the suggested equalities. These cases will meet in particular for the complex checkerwork that represents the vegetation of a zone of mixed-farming, for the small oases in arid zone, the clearings in the forest zones, for the edges of the massive forest or the maritime coasts. However, the suggested equations provide an approach for the problem.

II – ASSESSMENT Of ENERGY (*)

Suppose an uniformed system corresponding to the preceding conditions. During a period of 24 hours, the energy assessment brought to the unit of area is,

$$(1) \qquad (1-a)\,Rg + (1-a')\,Ra - a''\,\sigma T^4 + Q = E - C = ETR$$

the equation which gives the real evapotranspiration of the area considered. Thus, ETR more or less limited by the intervention of the factor "water" plays an essential part in the interaction of the physical data of the climate by these terms σT^4, Ra and in certain measurement Ra or even Rg.

ETP corresponds, by definition, in case the available energy is the only factor limiting the evaporation. Study the passage from ETR to ETP in the previously defined system. Let us indicate by ETP0 the value of the potential evapotranspiration when ETR is equal to ETP.

Suppose this condition to be realized

$$(2) \qquad ETR = ETP = ETP_0$$

Admit that for an independent reason of the energy phenomena, ETR decreases. This case could result in a period of dryness, of the maturity of vegetation, of its cut, etc…The reduction in ETR releases an energy q1 such as,

$$ETP_0 - ETR = q_1 . \tag{3}$$

With the scale considered, this modification of balance inside of the system does not affect the total radiation and only intervenes very slightly on the Ra term via the temperature and the moisture of the low atmospheric layers. The only important modification which will bring to the temperature and the turbulence, will cause a modification of ETP. Under the best conditions, i.e. if the transformation does not modify the exchanges of the system with outside, the energy returning available (q1) should correspond to an increase of ETP. Thus, without the modification of the initial climate from the energy point of view and in particular without the variation of the different primitive oasis effects, we will have

$$ETP = ETP_0 + q_1 \tag{4}$$

Where, by considering (3),

$$ETP + ETR = 2 ETP_0 \tag{5}$$

(*) We will admit as positive the energy received on the surface of the ground, as negative the energy lost. The following symbols will be used:

a --- albedo, the reflection fraction of the total radiation (expressed in percentage)
a' --- the reflection fraction of the atmospheric radiation
a" --- the emissivity
Rg --- the total radiation (the solar radiation ≤ 5μ received on an horizontal surface)
Ra --- the atmospheric radiation of the long wave > 5μ
σT^4 – the radiation of the ground at the absolute temperature T with an emissivity equal to the unit
E --- the energy involved by the evaporation
C --- the energy involved by the condensation
Q --- the energy exchanged by the conduction-convection by the considered system with outside
Qs --- the energy exchanged by the conduction in the ground
Qa --- the energy exchanged by the conduction-convection in the air. Qa comprises the exchange of heating of the various scales
ETR --- the energy corresponding to the real evapotranspiration
ETP --- the energy corresponding to the potential evapotranspiration

Thus, for a given climate, all would occur as if there were symmetry between ETR and ETP compared to a constant ETP0. Very generally, the transformation will not occur without the modification of the exchanges with outside and the equalities will transform themselves into inequalities.

$$(6) \qquad ETP + ETR \leqslant 2\,ETP_0$$

By using the equality (5) and by clarifying the values of Q according to the scales, the general equation (1) can be written as,

$$(7) \qquad ETP + (1-a)\,Rg + (1-a')\,Ra - a''\sigma T^4 + Qs + Q_3 + Q_{4.5} = 2\,ETP_0$$

(1 - a) Rg’, ETP0, $Q_{4.5}$ are not affected by the relative variation of ETR, and ETP related to the availability of the water. σT^4, Ra, Qs and even Q_3 are on the contrary variable. We can thus put (7) in the following form, by grouping the variable terms in a function g,

$$(8) \qquad ETP = 2\,ETP_0 + g - (1-a)\,Rg - Q_{4.5}$$

and according to (5),

$$(9) \qquad ETR = (1-a)\,Rg' + Q_{4.5} - g.$$

For the given values ETP0, Rg’, $Q_{4.5}$, ETR is a decreasing function of g, then ETP is an increasing function. When ETR = 0, ETP takes the maximum value corresponding to 2ETP0. Moreover, according to (9),

$$(10) \qquad g = (1-a)\,Rg' + Q_{4.5}$$

When the water is not a limiting factor, ETR becomes by definition equal to ETP. The variation of ETR explains then that of ETP. The maximum value likely to be taken under these conditions by ETR corresponds to the possible maximum value of ETP. According to (9), ETR will be maximal when g will be null. In fact, g that essentially represent the net radiation of the long wave (σT^4 - Ra), engine of night cooling, could not be positive, otherwise the night amplitude of the temperature would change the sign and the night temperatures would be increasing at night. We have then to the maximum the non limiting water with the factor,

$$(11) \qquad ETR_{\max} \text{ ou } ETP_{\max} = (1-a)\,Rg' + Q_{4.5}.$$

This maximum value of ETR or ETP under these conditions could not thus even be exceeded when ETR = 0. We have thus in this case,

$$(12) \qquad ETP \leqslant (1-a)\,Rg' + Q_{4,5}$$

where considering (5),

$$(13) \qquad 2\,ETP_0 \leqslant (1-a)\,Rg + Q_{4,5}$$

which gives,

$$(14) \qquad ETP_0 \leqslant 0{,}5[(1-a)\,Rg + Q_{4,5}].$$

We also deduce,

$$(15) \qquad ETP \leqslant g$$

or

$$(16) \qquad ETP \leqslant a\sigma'' T^4 - (1-a')\,Ra + Qs + Q_3.$$

The potential evapotranspiration can thus be expressed according to the radiative assessment of the long wave (σT^4 , R'a) in the measurement where the term (Q3) is not too large over a period of 24 hours. The equation (12) permits to understand how it is possible to relate ETP for a given place and certain duration of the day to the nychthemeral amplitude of temperature(the maximal temperature --- the minimal temperature) which is in relation to these exchanges of radiation of the long wave during the cooling phase of the night.

Finally, the equality ETR + ETP = 2 ETP0 is put in the form,

$$(15) \qquad ETR + ETP \leqslant (1-a)\,Rg + Q_{4,5}.$$

In addition, if we indicate by ε the ratio ETR/ETP,

$$(16) \qquad \varepsilon = \frac{ETR}{ETP}$$

εhas the meaning of an index of the relative evapotranspiration equal to 1 for the areas where ETR = ETP and equal to 0 for the desert areas.

The equation (13) permits then to express respectively ETP and ETR.

$$(15) \qquad ETP \leqslant \frac{(1-a)\,Rg + Q_{4.5}}{1+\varepsilon}$$

$$(16) \qquad ETR \leqslant \frac{\varepsilon[(1-a)\,Rg + Q_{4.5}]}{1+\varepsilon}$$

DISCUSSION

The potential evapotranspiration can thus be evaluated in two different ways over multiple periods of 24 hours when there are no important changes of temperature,

-- or from the radiation of long wave (σT^4 , Ra), which integrates via the temperature the oasis effects of great scale

--- or from the total absorptive radiation (1-a)Rg, the oasis effects of great scale (Q_4, Q_5) and of an index $\varepsilon$of the relative evapotranspiration.

ETP can not thus be defined only according to the energy factors independently from the water factor. We will study two limited cases:

When ε= 1

$$ETR = ETP \leqslant 0{,}5[(1-a)\,Rg + Q_{4.5}].$$

When ε= 0 ETR = 0

$$ETP \leqslant (1-a)\,Rg + Q_{4.5}.$$

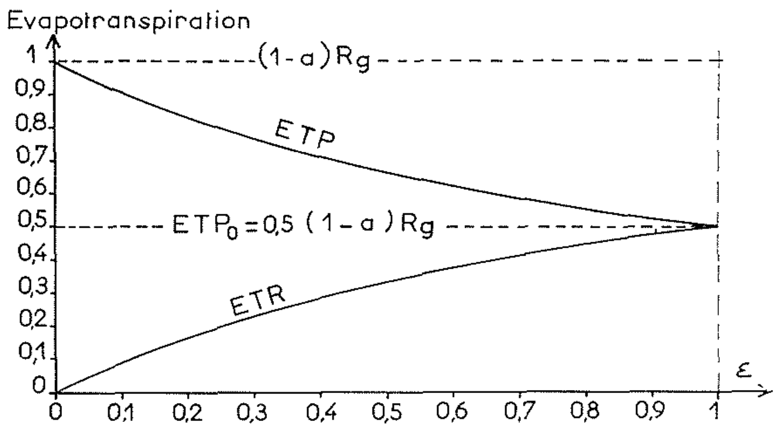

Fig. 2 – The possible maximal variation of ETR and ETP according to ε= ETR/ETP, the exchange of heating of great scale $Q_{4.5}$ being null

The potential evapotranspiration thus varies to the maximum between 2 limiting values from *2 ETPo = (1 - a) Rg + Q4.5* to ETP0 = 0,5[(1 -a)Rg+ Q4.5] when ETR varies from 0 to ETP. The figure 2 gives the variation of ETR and ETP according to $\varepsilon$when the oasis effects of great scale are negligible.

Thus, for the equatorial zones where we can admit $\varepsilon = 1$, ETP should be inferior or equal to $(1 - a)$ Rg. Hydrous assessments of some river basins provided by L. TURKISH emphasize an annual ETP about half of the radiation total suitable for be absorbed by an abundant and wet foliage. The hydrous assessments of some river basins provided by L. TURC emphasize an annual ETP in order of the half of the total radiation likely to be absorbed by an abundant and wet foliage.

The same conclusion would be valid for the very large stretches of water such as the seas. However, in the vicinity of the coasts, we will have to take into account of the disturbances introduced by the "calorific wheels" different from the ground and the sea which systematically produce the oasis effects in the form of breeze of sea and of ground of scale equal to or higher than e3. These side exchanges are still increasing with the vicinity of the desert coasts.

If we consider a zone strongly sprinkled such as a very vast oasis in a desert, we can admit that on the edge, we are under the conditions of the desert climate ETR = 0, whereas in center ETR is equal to ETP. Thus from the edge to the center, we can justify from the preceding equations a variation which is from simple to double, all other conditions remaining equal, according to the importance of the guard ring placed around to standardize the conditions. If the preceding inequalities do not give the variation of ETP according to the distance of the considered perimeter, they make it possible to define the higher and lower limits and to find by a very different way, the curves of SUTTON, taken again by CALDER, DUFFEL and LATTAN on the reduction of ETP according to the guard ring (Fig. 3).

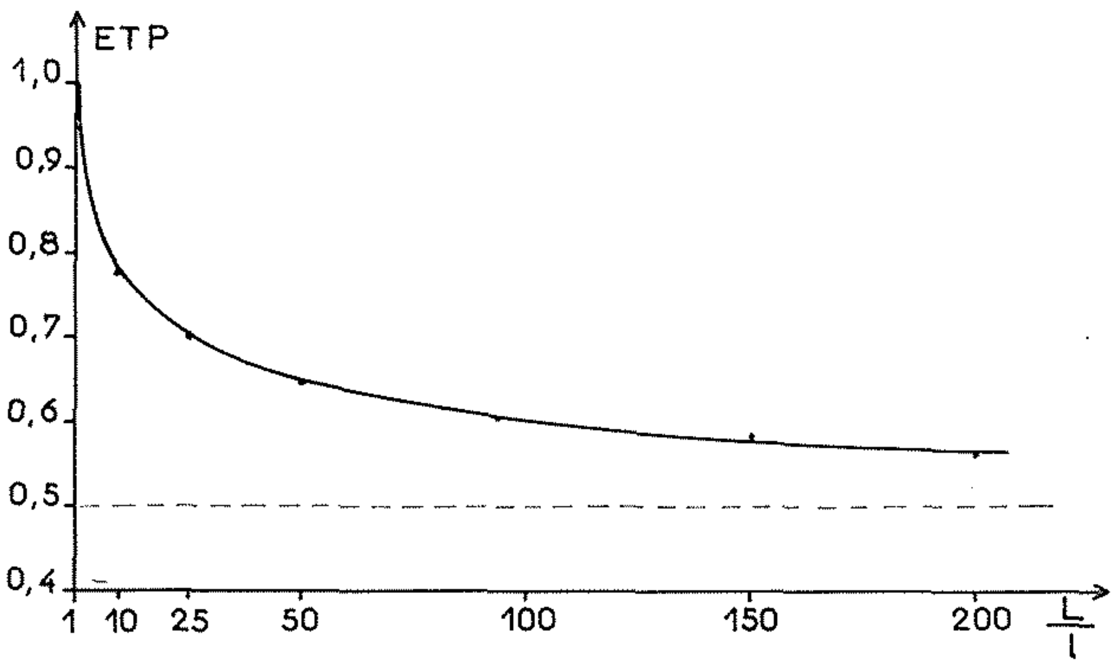

Fig. 3 - The variation of ETP according to the ratio L/l from the radiation of the guard ring to that of the measured zone giving ETP.

It will be noted that in an area of mixed-farming, the ETR are very different from each other. This result that ETP will be itself different; but the oasis effects will have, for the effect trending to standardize them, certain zones used as the relatively hot sources, others as the relatively cold sources. According to the importance of the surfaces, the oasis effects will raise different scales. ETP will not only correspond to the average value at the scale superior to that of the turbulence which will not translate ETP of the more reduced surfaces, since it will correspond to the average ETR of the same zone and not ETR of each field.

The preceding whole of the equations supposes that when we pass from ETP to ETR, the transformation is done without perturbing the previous climate. This reasoning is valid only at the limit and will all the more far from the reality, because the ratio between ETR and ETP will vary quickly in the time, or its uniformity zone will possess the dimensions far from the ones corresponding to the scale that defines the climate. Nevertheless, if we consider an uniform zone sufficiently extensive, they allow to define the limits of possible variation of ETR or ETP all linking to the different terms of the assessment *(Rg,* Rnet of the long wave).

Note that the water provision of irrigation has an effect on lowering ETP while highing ETR. This double action contributes to improve strongly the vegetable production. This lowering of ETP, all other conditions remaining equal, will be all the more marked since the treated surface will be important. However, we note that to consider, in a very dry region, ETR as the neighbor of ETP, it will be necessary to irrigate the surface having a very high scale superior to e2. It's thus about a surface corresponding to several Km^2 (several hundreds of hectares). In this case, it will be possible to lower strongly ETP and when the scale of the surfaces grows, one will be able to consider the limit, and to arrive at dividing ETP by two. This decrease of ETP for the high scale corresponds not only to a reduction of water consumption, but also to an important improvement of its efficiency.

CONCLUSION

The study of the energy assessment of an uniform region (ground, vegetable cover, nutrition in water) done during a period of 24 hours, allows to establish the simple relations between the real and potential évapotranspiration and the terms of the energy assessment *(Rg, Rnet of the long wave*). These relations were established with a series of hypotheses that we do not meet generally in the natural conditions; they provide, however, an approach of ETR and of ETP and emphasis the role played by the totally absorbed radiation. The existing compensation between ETP and ETR translated by simple relation ETP + ETR equal to constant for a certain totally absorbed radiation, allows to explain the variations of ETP from these of ETR. We then can have an indication on the order of magnitude of the climatic modifications that we can await of a change of the vegetable cover or of a water provision by carrying out the irrigation to a sufficient scale.

TABLE 2

Real Evapotranspiration (ETR) in the Equatorial zone

I --- observed values --- Extract of the thesis of L. TURC "The water assessment of the grounds --- relations amongthe precipitations, the evaporation and the flow"

Current water, with eventually the surface of the pouring basin and the period of doing the report	Rain in mm	0°C	ETR
a) Java			
Tji Anten (240 km2) 17 years	4.935 mm	21°	1.188 mm
Tji Kapundung	2.650 mm	18°	1.070 mm
b) South America			
Amazone (report not known)	1.900 mm	24° 5	1.245 mm
c) Africa			
Congo (report not known)	1.400 mm	22° 5	1.030 mm
Sanaga à Edea	1.610 mm	23°	1.095 mm

II --- Maximum theoretical values of annual ETR

Total Radiation (Annual average expressed in cal /cm2 /day)	Albedo	
	5%	10%
350	1.040 mm	990 mm
400	1.190 mm	1.130 mm
450	1.340 mm	1.270 mm

The theoretical maximum values of annual ETR were calculated from the equality $ETR = ETP = ETP0 = 0,5\ (1 \sim a)Rg \times 365$.

The albedo 5% and 10% can correspond to those from a dense forest to the humid foliage.

At which time scale does the complementary principle perform best on evaporation estimation?

Liming Wang[1], Songjun Han[2], Fuqiang Tian[1*].

[1] Department of Hydraulic Engineering, State Key Laboratory of Hydroscience and Engineering, Tsinghua University, Beijing 100084, China

[2] State Key Laboratory of Simulation and Regulation of Water Cycle in River Basin, China Institute of Water Resources and Hydropower Research, Beijing 100038, China

Correspondence to:

Fuqiang Tian: tianfq@mail.tsinghua.edu.cn

Abstract

The complementary principle has been widely used to estimate evaporation under different conditions. However, it remains unclear ~~that~~ at which time scale the complementary principle performs best. In this study, evaporation estimations ~~was~~ were conducted~~assessed over~~ at 88 eddy covariance (EC) monitoring sites at multiple time scales (daily, weekly, monthly, and yearly) by using ~~the~~ sigmoid and polynomial generalized complementary functions. The results indicate that the generalized complementary functions exhibit the highest skill in estimating evaporation at the monthly scale. The uncertainty analysis shows that this conclusion is not affected by ecosystem type~~s~~ ~~nor~~ or energy balance closure method~~energy correction methods~~. Through comparisons at multiple time scales, we found that the slight difference between the two generalized complementary functions only exists when the independent variable (*x*) in the functions approaches 1. The ~~difference~~ results differ ~~in different performance of~~for the two models at daily and weekly scales. However, such differences vanish~~es~~ at monthly and annual time scales ~~as~~ with few high *x* values occurring~~occurrences~~. This study demonstrates the applicability of ~~the~~ generalized complementary functions across multiple time scales and provides a reference for choosing ~~the~~ a suitable timestep for evaporation estimations in relevant studies.

Keywords:

Evaporation; Generalized complementary functions; Multiple time scales; Ecosystem types~~;~~ ~~Energy correction methods~~

1. Introduction

Terrestrial evaporation (E) including soil evaporation, wet canopy evaporation, and plant transpiration, is one of the most important components in the global water ~~and energy~~ cycle~~s~~ and energy balance (Wang and Dickinson, 2012). The evaporation process affects the atmosphere through~~by~~ a series of feedbacks involving~~on~~ humidity, temperature, and momentum (Brubaker and Entekhabi, 1996; Neelin et al., 1987; Shukla and Mintz, 1982). Quantifying evaporation is crucial for a deep understanding of water and energy interactions between the land surface and the atmosphere. Generally, ~~the~~ meteorological studies focus on ~~the~~ evaporation changes at hourly and daily scales; ~~the~~ hydrological applications require~~need~~ evaporation data at weekly, monthly or longer time scales (Morton, 1983); and ~~the~~ climate change studies~~researches~~ focus~~pay~~ more ~~attention to the~~on interannual variations. The observation of E can occur~~be operated~~ at different time scales. For example, the e~~E~~ddy covariance, lysimeter, and scintillometer can measure ~~the~~ evaporation at the half-hour scale, and ~~the~~ water balance methods can observe ~~the~~ evaporation at monthly to yearly scales (Wang and Dickinson, 2012). However, in most situations, an~~the~~ observation is unavailable, and the estimation of E is necessary. There are several types of methods for evaporation estimations, for example, the Budyko-type methods (Budyko, 1974; Fu, 1981), the Penman-type methods (Penman, 1948; Monteith, 1965) and the complementary-type methods (Bouchet, 1963; Brutsaert and Stricker, 1979). The Budyko-type methods perform well at annual or longer time scales; the Penman-type methods can be applied at hourly and daily scales,~~;~~ while the complementary-type methods are used at multiple time scales (Crago and Crowley, 2005; Han and Tian, 2018; Crago and Crowley, 2018; Ma et al., 2019) without ~~an~~ explicit consideration of~~cognization of~~ the time scale issue.

Recently, the complementary principle, as one of the major types of E estimation methods, has drawn increasing attention because it can be implemented with standard meteorological data (radiation, wind speed, air temperature, and humidity) without ~~the requirement for~~ complicated underlying surface properties. Based on the coupling between the land surface and the atmosphere, the complementary principle assumes that the limitation of the wetness state in the underlying surface on evaporation can be synthetically reflected by ~~the~~ atmospheric wetness (Han et al., 2020). Bouchet (1963) first proposed the "complementary relationship" (CR), which suggested that ~~the~~ apparent potential evaporation (E_{pa}) and ~~the~~ actual E depart from potential evaporation (E_{po}) in equal absolute values but opposite directions ($E_{pa} - E_{po} = E_{po} - E$). According to the Advection–Aridity approach (AA, Brutsaert and Stricker, 1979), E_{pa} is formulated by Penman's (1948) equation (E_{pen}), and E_{po} is formulated by Priestley-Taylor's (1972) equation (E_{PT}). Subsequently, the CR was extended to a linear function with an asymmetric parameter (Brutsaert and Parlange, 1998). Further studies have found that the linear function underestimates E in arid environments and overestimates E in wet environments (Han et al., 2008; Hobbins et al., 2001; Qualls and Gultekin, 1997). To address thise issue, Han et al. (2011; 2012; 2018) proposed a sigmoid generalized complementary function (SGC, see equation (1) for details). As a modification to the AA approach, the SGC function illustrates the relationship between two dimensionless terms, E/E_{pen} and E_{rad}/E_{pen}, where E_{pen} is ~~the~~ Penman evaporation (Penman, 1948) and E_{rad} is the radiation term of E_{pen}. The SGC function shows higher accuracy in estimating E (Han and Tian, 2018; Ma et al., 2015b; Zhou et al., 2020) and outperforms the linear functions, especially in dry desert regions and wet farmlands (Han et al., 2012). Obtaining the impetus from Han et al. (2012), Brutsaert (2015) proposed a quartic polynomial generalized complementary function (PGC, see equation (5) for detail). The PGC function describes the relationship between E/E_{pa} and E_{po}/E_{pa}, where E_{pa} and E_{po} are formulated in the manner of the AA approach. The PGC function has also been frequently used in recent years (Brutsaert et al., 2017; Hu et al., 2018; Liu et al., 2016; Zhang et al., 2017).

The prerequisite of the complementary principle is ~~the~~ adequate feedback between the land surface and the atmosphere, which results in an equilibrium state. In this situation, the wetness condition of the land surface can be largely represented by the atmospheric conditions. Therefore, the time scales used in the complementary principle need to satisfy the adequate feedback assumption. However, this issue involves the complex processes of atmospheric horizontal and vertical motion, and these processes are~~it is~~ difficult to ~~be explained~~explain theoretically. Morton (1983) not~~ic~~ed this problem earlier and suggested that the complementary principle is not suitable for short time scales (e.g., less than 3 days) mainly because of the potential lag times associated with the response of energy and water vapor storage to disturbances in the atmospheric boundary layer. However, there is no solid evidence or theoretical identification to support this inference. The original complementary relationship and the AA function are not limited by ~~the~~ applicable time scales. In the derivation of the advanced generalized complementary functions (SGC of Han and Tian (2018) and PGC of Brutsaert (2015)), no specific time scale is defined~~ neither~~. In practice, the complementary principle has been widely adopted to estimate E at multiple time scales, including hourly (Crago and Crowley, 2005; Parlange and Katul, 1992), daily (Han and Tian, 2018; Ma et al, 2015b), monthly (Ma et al, 2019; Brutsaert, 2019), and annual scales (Hobbins et al., 2004). The accuracy of the results have varied in different studies. Crago and Crowley (2005) found that the linear complementary function performs well in estimating *E* at small time scales of less than half-hour using the data from several well-known~~famous~~ experimental projects (e.g., International Satellite Land Surface Climatology Project). The correlation coefficient between simulated *E* and observed *E* ranges from 0.87 to 0.92 in different experiments. The results of Ma et al. (2015b) indicated that the SGC function (Root-Mean-Square Error, RMSE = 0.39 mm day^{-1}) performs well~~is competent~~ in estimating *E* in an alpine steppe region of the Tibetan Plateau at the daily scale. Han and Tian (2018) applied the SGC function to~~on~~ the daily data of 20 EC sites from~~ the~~ FLUXNET and found that it performed~~s~~ well in estimating *E* with a mean Nash-Sutcliffe efficiency (NSE) value of 0.66. Crago and Qualls (2018) evaluated the PGC function and their rescaled complementary functions using the weekly data of 7 FLUXNET sites in Australia, and the results showed that all the functions performed adequately with a correlation coefficient between simulated *E* and observed *E* higher than 0.9. Ma et al. (2019) also validated an emendatory polynomial complementary function at the monthly scale, and the NSE values of 13 EC sites in China ~~are~~ were higher than 0.72. At the annual scale, Zhou et al. (2020) found that the mean NSE of the SGC function ~~is~~ was 0.28 for 15 catchments in the Loess Plateau. Since these results were derived with different functions under varied conditions, it is difficult to determine at which time scale the performance is the best, and it is more difficult to explain theoretically how long the land-atmosphere feedback needs to achieve equilibrium.

In previous studies, the model validations were mostly completed at the daily scale (Brutsaert, 2017; Han and Tian 2018; Wang et al. 2020), and the datasets of evaporation estimation were often established at the monthly scale (Ma et al., 2019; Brutsaert et al., 2019). However, each study only focused on a single timescale. In this study, we assessed the performance of the complementary functions on evaporation estimation at multiple time scales (daily, weekly, monthly, and yearly). The assessment was carried out ~~over~~ at 88 EC monitoring sites with > 5-year-long observation records. In view of the fact that the complementary principle has developed to the nonlinear generalized forms, we selected two nonlinear complementary functions in the literature, i.e., the SGC function (Han et al., 2012; 2018) and the PGC function (Brutsaert, 2015). The key parameters of the complementary functions need to be determined by calibration. We chose the uniform database and the uniform parameter calibration methods for the optimization of the two complementary functions. We aimed to determine the most suitable timescale for the complementary functions through a comparison of the performances at different timescales. It’s important for not only ~~for the~~a deep understanding of the application of the complementary principle~~,~~ but also ~~for the~~ timestep selection in ~~the~~ evaporation database establishment and evaporation trend analysis.

This paper is organized as follows:~~.~~ Section 1 briefly describes the development of the complementary theory and our motivations to investigate the timescale issue. Section 2 describes the two functions, the parameter calibration method, and the data sources and processing. Section 3 shows and discusses the performance of the complementary functions at multiple time scales, the dependence of the key parameters on time scales, and the uncertainties in the analysis. The conclusions are given in Section 4.

2. Methodology

2.1 ~~The s~~Sigmoid generalized complementary function

Han et al. (2012; 2018) proposed a generalized form of the complementary function that expresses E/E_{pen} as a sigmoid function (SGC) of $E_{\mathrm{rad}}/E_{\mathrm{pen}}$:

$$y = \frac{E}{E_{Pen}} = \frac{1}{1 + m\left(\frac{x_{max} - x}{x - x_{min}}\right)^{n}}$$

$$x = \frac{E_{rad}}{E_{Pen}} \tag{1}$$

where x_{max} corresponds to the certain maximum value of x under extremely wet environments, and x_{min} corresponds to the certain minimum value of x under extremely arid environments. In this study, x_{max} and x_{min} were set as 1 and 0, respectively, for convenience. The E_{pen} term is defined by Penman's equation (Penman, 1950; Penman, 1948), which can be expressed as:

$$E_{pen} = \frac{\Delta(R_n - G)}{\Delta + \gamma} + \frac{\rho c_p}{\Delta + \gamma} \frac{\kappa^2 u}{ln(\frac{z - d_0}{z_{0m}})\, ln(\frac{z - d_0}{z_{0v}})} (e_a{}^{*} - e_a) \tag{2}$$

where, Δ (kPa C^{-1}) is the slope of the saturation vapor curve at air temperature; R_n is the net radiation; G is the ground heat flux; γ (kPa C^{-1}) is a psychrometric constant; ρ is the air density; c_p is the specific heat; $\kappa = 0.4$ is the von Karman constant; u is the wind speed at measurement height; $e_a{}^{*}$ and e_a are the saturated and actual vapor pressures of air, respectively; z is the measurement height (Table S1); d_0 is the displacement height; z_{0m} and z_{0v} are the roughness lengths for momentum and water vapor, respectively, which are estimated from the canopy height (h_c, Table S1), $d_0 = 0.67h_c$, $z_{0m} = 0.123h_c$, and $z_{0v} = 0.1z_{0m}$ (Monin and Obukhov, 1954; Allen et al., 1998). E_{rad} is the radiation term of ~~the~~ Penman evaporation:

$$E_{rad} = \frac{\Delta(R_n - G)}{\Delta + \gamma} \tag{3}$$

The two parameters *m* and *n* of equation (1) can be determined by the Priestley-Taylor coefficient *α* and the asymmetric parameter *b* (Han and Tian, 2018).

$$\begin{cases} n = 4\alpha(1 + b^{-1})x_{0.5}(1 - x_{0.5}) \\ m = (\frac{x_{0.5}}{1 - x_{0.5}})^n \end{cases} \tag{4}$$

where, $x_{0.5}$ is a variable that corresponds to $y = 0.5$~~,~~ and equals ~~to~~ $\frac{0.5+b^{-1}}{\alpha(1+b^{-1})}$.

2.2 ~~The p~~Polynomial generalized complementary function

Brutsaert (2015) proposed the polynomial generalized complementary (PGC) function, which describes the relationship between E/E_{pa} and E_{po}/E_{pa}. We uniformed the independent variable as E_{rad}/E_{pen} to compare the two functions conveniently, and the polynomial function can be expressed as:

$$y = (2 - c)\alpha^2x^2 - (1 - 2c)\alpha^3x^3 - c\alpha^4x^4 \tag{5}$$

where, *c* is an adjustable parameter. When $c = 0$, equation (5) reduce to

$$y = 2\alpha^2x^2 - \alpha^3x^3 \tag{6}$$

2.3 Parameter optimization method

Typically, *α* has a default value of 1.26 (Priestley & Taylor, 1972). Since some studies have shown that a constant *α* may cause illogical results and biases in estimating *E*, it is suggested to specify α for diverse scenarios (Hobbins, Ramírez, Brown, & Claessens, 2001; Ma et al., 2015a; Sugita et al., 2001; Szilagyi, 2007). According to the complementary principle, under wet conditions, E is close to E_{pen} and the Priestley-Taylor's evaporation ($E_{PT} = \alpha\, E_{rad}$). Specifically, when E/E_{pen} is larger than a threshold (0.9 is commonly adopted), E_{PT} can be considered to be approximately equal to the observed E; thus, α can be calculated by E/E_{rad} (Kahler and Brutsaert, 2006; Ma et al., 2015a). In this study, α was calculated by this method based on the mean value of E/E_{rad} under wet conditions ($E/E_{pen} > 0.9$). ~~In this study, α was calculated by the mean value of E/E_{rad} whenever E/E_{pen} is larger than 0.9 (Kahler and Brutsaert, 2006; Ma et al., 2015a).~~ When all the E/E_{pen} values are less than 0.9, α was set as the default value of 1.26. The key parameter b in SGC was calibrated by an optimization algorithm with the objective function as the minimization of the mean absolute error (MAE) between the estimated E (by equation (1)) and the observed E. Similarly, the key parameter c in PGC was calibrated by an optimization algorithm with the objective function as the minimization of the MAE between the estimated E (by equation (5)) and the observed E. Since we used the optimization algorithm to determine the parameter b in the SGC function, it is a fair manner to use the optimal c value instead of a constant value ($c = 0$) in the PGC function.

To make the model parsimonious, we gave one value for the parameters (α, b and c) at each site for every different time scale. If the parameter was alterable, for example, it was monthly dependent, and we would have to calibrate 12 parameters instead of one value for the whole study period. The purpose of this study is to determine the most suitable timescale for the complementary functions, and the variances of the key parameter within a timescale will introduce extra uncertainties. The accuracy will increase when an alterable parameter (that means a higher number of parameters) is used; however, the probability of overfitting risk will increase at the same time. In addition, in comparison to a group of parameters, a general representation of the parameter is more helpful in detecting its overall trend as the change in the timescale.

2.4 Data sources and data processing

The eddy flux data analyzed in this study were obtained from the FLUXNET database (http://fluxnet.fluxdata.org, Baldocchi et al., 2001). Observations from a total of 88 sites around the world were analyzed. ~~The d~~Detailed information on these sites is listed in Table S1. These sites were selected from the FLUXNET database because they have observations ~~for~~ longer than 5 years. The 88 sites include 11 IGBP (International Geosphere-Biosphere Programme) land cover classes: ENF, evergreen needleleaf forests (27 sites); EBF, evergreen broadleaf forests (8); DBF, deciduous broadleaf forests (13); MF, mixed forests (5); OSH, open shrublands (4); CSH, closed shrublands (1); WSA, woody savannas (3); SAV, savannas (4); GRA, grasslands (15); CRO, croplands (6); and WET, permanent wetlands (2). The climates of the 88 sites range~~s~~ from arid to humid. Among the 88 sites, 11 sites have mean annual precipitation levels lower than 200 mm, 47 sites have precipitation levels between 200 ~ 500 mm, and 30 sites have precipitation levels above 500 mm. Eleven sites are located in the Southern Hemisphere (i.e., Australia, Brazil, and South Africa) and the others are located in the Northern Hemisphere.

Variables including net radiation, sensible heat flux, latent heat flux, ground heat flux, wind speed, air temperature, air pressure, precipitation, relative humidity, and vapor pressure deficit were acquired from the daily, weekly, and monthly datasets on the FLUXNET website. We analyzed the observations in the growing seasons from April to September for the Northern Hemisphere and from October to March for the Southern Hemisphere. These study periods were selected to avoid the high biases caused by the low level of~~small~~ solar radiation or ~~the~~ extremely low evaporation (≈ 0) during the nongrowing season. The seasonal and annual data were acquired by averaging the monthly data of the growing seasons. Following Ershadi et al. (2014), the energy residual corrected latent heat fluxes were used, which means the residual term in the energy balance is attributed to the latent heat to force the energy balance closure. To investigate the influence of different residual correction methods, the Bowen ratio energy balance method was also adopted in the uncertainty analysis. In the Bowen ratio method, the residual term is attributed ~~in~~to sensible heat and latent heat by preserving the Bowen ratio (Twine et al., 2000). The latent heat, sensible heat, and available energy ($R_n - G$) ~~were~~ are restricted to positive values (Han and Tian, 2018). The energy balance residual (W m^{-2}) and energy balance closure ratio for each site are shown in Table S1.

The Nash-Sutcliffe efficiency (NSE, Legates and McCabe, 1999) is used to evaluate the efficiency of estimating E by the two generalized complementary functions:

$$\mathrm{NSE} = 1 - \frac{\sum(E - E_{est})^2}{\sum(E - \bar{E})^2} \tag{7}$$

where, E_{est} (W m^{-2}) is the estimated evaporation according to equation (1) or equation (5) and $\bar{E}$ is the mean value of E (W m^{-2}).

3. Results and discussion

3.1 Performance of the SGC function at multiple time scales

The relationship between the estimated E_{est} (site mean values) based on the SGC function (equation (1)) and the observed E at~~of~~ the 88 sites at multiple time scales is shown in Figure 1. The regression equations and determination coefficients (R^2) were calculated by the site mean results. Each dot in Figure 1 represents the site mean result averaged by daily (Figure 1a), weekly (Figure 1b), monthly (Figure 1c), and yearly (Figure 1d) results, and the total observation number is 88 (sites) at each timescale. Most of the results ~~lie~~ are near the 1:1 line, and all the regression slopes are close to 1 with high R^2 (0.95 ~ 0.99), which means the sigmoid function exhibits a good performance in estimating ~~to estimate~~ E at multiple time scales. ~~The interceptions range from −1.69 to 2 W m^{-2}. All the coefficients of the regression show indistinctive differences at different time scales. However, t~~The evaluation merits show that the performance varies at each time scale. The NSE values of the SGC functions for each site at different time scales are listed in Table S2. For the 88 sites, nearly half of the sites (40) have the highest NSE at the monthly scale, 12 sites have the highest NSE at the daily scale, 13 sites have the highest NSE at the weekly scale, and 23 sites have the highest NSE at the annual scale. The mean results of NSE_H, R^2_H, and $RMSE_H$ (the subscript H corresponds to the sigmoid function proposed in Han and Tian, 2018) of these sites are shown in Table 1. R^2_H represents the mean value averaged by the determination coefficients within each site. When the timescale changes from day to month, the mean NSE_H increases from 0.33 to 0.55, and R^2_H also increases from 0.61 to 0.75 (Table 1). However, they both decrease at the annual scale (NSE_H = 0.18 and R^2_H = 0.61). These results indicate that the SGC function exhibits the highest skill at the monthly scale. We inferred that there is a tradeoff between the random error and the number of observations. $RMSE_H$ values decrease from 24.56 W m^{-2} at the daily scale to 7.33 W m^{-2} at the annual scale, which means that the random error decreases as the time scale increases. At the same time, the fewer observations at the annual scale result in decreased variabilities of *x* and *y*, which affect the performance of the SGC function. On the other hand, Morton (1983) did not suggest using the complementary principle for short time intervals (e.g., less than 3 days), mainly considering the lag times associated with heat and water vapor change in the atmosphere, which ~~can~~ may provide a possible ~~explain~~inference for the weak performance at the daily scale ~~that the weekly and monthly results are better than the daily results~~.

In previous studies, the SGC function was mainly applied at the daily scale. For example, the results of Ma et al. (2015b) in the alpine steppe region showed that the NSE of the sigmoid function is 0.26 at the daily scale, which is lower than our mean value in the grassland (0.73 ± 0.08). The RMSE (11.06 W m^{-2}) is smaller than ours (16.36 ± 1.48 W m^{-2}). The mean NSE of the 20 EC sites from ~~the~~ FLUXNET is 0.66 at the daily scale in Han and Tian (2018), approximately~~about~~ two times ~~of~~ the result in this study, and the RMSE (18.6 ± 0.94 W m^{-2}) is lower than our mean result of 88 sites (24.56 ± 0.95 W m^{-2}).

The SGC function for the five selected sites of different ecosystem types is shown in Figure 2 to show the performance at multiple time scales (red lines in Figure 2). These five EC monitoring sites were selected because they have long-~~period~~ term observations (> 10 years). The five sites include an evergreen needle forest (CA-TP1, Figures 2(a) to (d)), a deciduous broad forest (US-UMB, Figures 2(e) to (h)), a woody savanna (US-SRM. Figures 2(i) to (l)), a cropland (US-Ne2, Figures 2(m) to (p)) and a grassland (US-Wkg, Figures 2(q) to (t)). As observations decrease from the daily to the annual scale, the results converge on the middle part of the sigmoid curves and lie closer to the fitted lines. For some sites, the annual results concentrate on a narrow range with lower annual variabilities (e.g., Figures 2(h), 2(l) & 2(t)). Generally, the key parameter (b) of the SGC function at these sites increases from the daily scale to the annual scale, which indicates that the sigmoid curves in the two-dimensional space of E_{rad}/E_{pen}-E/E_{pen} move upwards. ~~The~~ A detailed discussion about the variation ~~of~~ in the parameters is provided~~elaborated~~ in Section 3.4.

3.2 Performance of the PGC function at multiple time scales

The relationship between the estimated E_{est} (site mean values) based on the PGC function (equation (5)) and the observed E ~~of~~ at the 88 sites at multiple time scales is shown in Figure 3. The slopes of the regression increase from 0.9 to 1 as the timescale changes from day to month~~,~~ and further increase to 1.01 at the annual scale. The intercept terms decrease from 13.06 W m^{-2} at the daily scale to 0.01 W m^{-2} at the monthly scale~~,~~ and further decrease to −0.25 W m^{-2} at the annual scale. The R^2 values increase from 0.83 to 0.99 as the time scale increases. These coefficients of the regression show that the PGC function exhibits the highest skill at the monthly scale. The NSE values of the PGC functions for each site at different time scales are listed in Table S2. For the 88 sites, 42 sites have the highest NSE at the monthly scale, 7 sites have the highest NSE at the daily scale, 14 sites have the highest NSE at the weekly scale, and 25 sites have the highest NSE at the annual scale. The mean values of NSE_B, R^2_B, and $RMSE_B$ (the subscript B corresponds to the polynomial function proposed in Brutsaert, 2015) of these sites are shown in Table 1. When the timescale changes from day to month, NSE_B increases from 0.19 to 0.50, and R^2_B increases from 0.61 to 0.75. They decrease at the annual scale (NSE = 0.25 and R^2_H = 0.63). Again, these evaluation merits indicate that the PGC function also exhibits the highest skill at the monthly scale, which is the same as for the SGC function.

The PGC function has been applied at multiple time scales in previous studies. Zhang et al. (2017) evaluated the performance of the PGC function in estimating evaporation at 4 EC flux sites located across Australia, and their results showed that the mean RMSE (24.67 W m^{-2}) and R^2 (0.65) are close to our results (RMSE = 26.83 ± 1.16 W m^{-2} and R^2 = 0.61) at the daily scale. In Crago and Qualls (2018), the mean RMSE of 7 EC sites at the weekly scale ~~is~~ was 20.6 W m^{-2} and the mean R^2 ~~is~~ was 0.81, which are close to our mean results (RMSE = 19.17 ± 0.95 W m^{-2} and R^2 = 0.7).

The PGC functions for the five selected sites are also shown in Figure 2 (green lines). The fitted lines are almost the same as~~duplicate with~~ those of the SGC function in most situations when x is not too high. However, they diverge from each other when x becomes larger.

Finally, y exceeds 1 when x is larger than $1/\alpha$. Generally, the key parameter (c) of the PGC function at these sites decreases from the daily scale to the annual scale, which also indicates that the fitted curves move upwards.

3.3 Performance comparison of the SGC and PGC functions

The results ~~of~~ from the 88 sites (Figure 1, Figure 3 and Table 1) show that the performances of the two functions are similar at monthly and annual time scales, while the SGC function performs slightly better than the PGC function at daily and weekly time scales. According to the results in Figure 2, ~~it can be recognized that~~ the two functions with calibrated parameters are approximately identical under non-humid environments, but their difference increases as x (E_{rad}/E_{pen}) increases. We found that the values of α for all sites are greater than 1.0 in our study, which means that the PGC model cannot work properly under the condition of $1/\alpha < E_{rad}/E_{pen} < 1.0$. At daily and weekly time scales, ~~quite~~ a substantial number of~~few~~ ecosystems can produce very high E_{rad}/E_{pen} values. Specifically, 63 of the 88 sites have high E_{rad}/E_{pen} values ($x > 1/\alpha$) at the daily scale, and 24 sites have high values at the weekly scale. However, there are only 3 sites with an $x > 1/\alpha$ at the monthly scale, and no site has that value at the yearly scale. For the SGC function, in super humid conditions, the upper part of the sigmoid curve is nearly flat and closer to the observations (e.g., Figures 2 (a), (m) & (n)). However, for the PGC function, theoretically, it cannot be applied when x is over $1/\alpha$ because the estimated E_{est} will be higher than E_{pen}, which is illogical~~irrational~~. Thus, the sigmoid function performs slightly better at daily and weekly time scales than the polynomial function. However,~~But~~ the difference vanishes~~d~~ at the monthly scale as few high E_{rad}/E_{pen}

values occur~~occurrences~~.

According to the results, the performance of the PGC function ~~acts~~ is more sensitive to the timestep than that of the SGC function. On the one hand, the regression relationship between E_{est} and the observed E of the 88 sites shows that the performance of the SGC function remains more stable (Figure 1), while the regression results of the PGC function have higher variation when the time scale changes (Figure 3). On the other hand, the estimation merits (Table 1) further confirm the sensitivity of the PGC function. From the daily scale to the monthly scale, the increase ~~of~~ in NSE_H is 0.22, while the increase ~~of~~ in NSE_B is 0.31; $RMSE_H$ decreases by 11.36 W m^{-2} (46%), and $RMSE_B$ decreases by 13.13 W m^{-2} (49%). At the daily scale, quite a few ecosystems (63 of 88 sites) can experience frequent high E_{rad}/E_{pen} ($> 1/\alpha$) values~~occurrences~~, and the PGC function does not have the ability to simulate E accurately in this situation ($E_{est} > E_{pen}$) resulting in lower efficiency. We have carried out an additional analysis that adopts $E = E_{pen}$ for $1/\alpha < E_{rad}/E_{pen} < 1.0$ in the PGC function, and the resultant NSE_B (0.19 vs 0.19) and $RMSE_B$ (26.83 W m^{-2} vs 26.68 W m^{-2}) present very similar results. As the time scale increases, the results converge on the middle part of the fitted line, and the number of high x greatly decreases~~reduces~~ (Figure 2). Thus, the efficiency of the PGC function obviously increases~~obviously~~. This is~~It's~~ the reason that the polynomial function acts more sensitive to the timestep.

In addition, we found that the two complementary functions perform reasonably well at shorter timescales (i.e., day and week) with relatively high R^2 values. Additionally, the estimations of site mean evaporation at shorter timescales are accurate (Figure 1 and Figure 3), especially for the SGC function. These results suggest that the generalized complementary functions have the ability to estimate evaporation accurately even at shorter timescales.

3.4 Dependence of the key parameters of the SGC and PGC functions on time scales

The key parameters of the two complementary functions (b of the SGC function and c of the PGC function) vary at multiple time scales (Figure 2). To explore their changes, the values of $1/b$ and c ~~of~~ at the 88 sites were averaged at each timescale. To take into account ~~of~~ the situation in which~~that~~ b is equal to infinity, we used $1/b$ instead of b in this analysis. Figure 4 shows the change in~~of~~ the two complementary functions with varied parameters at multiple time scales. The averaged $1/b$ decreases from 0.45 ± 0.05 at the daily scale to 0.24 ± 0.03 at the annual scale (Figure 4a), and the averaged c decreases from 0.98 ± 0.19 at the daily scale (Figure 4b) to −0.37 ± 0.22 at the annual scale. The sign of c changes from positive to negative at the monthly scale.

We show~~ed~~ the histograms of $1/b$ and c at multiple time scales in Figure 5 and Figure 6, respectively. At the daily scale, half of the $1/b$ values are lower than 0.3, and the mean value is 0.45 ± 0.05. At the weekly scale, the peak of the distribution moves left, and almost~~nearly~~ half of the $1/b$ values are lower than 0.2 with ~~the~~ a mean value of 0.36 ± 0.04. At the monthly scale, the mean value is 0.29 ± 0.04, and the $1/b$ values continue to decrease. At the annual scale, the mean value decreases to 0.24 ± 0.03, and 61% of the $1/b$ values are lower than 0.2. According to Figure 6, at the daily scale, c follows a normal distribution (p-value = 0.17, Kolmogorov-Smirnov test) with ~~the~~ a mean value of 0.98 ± 0.21. Nearly 1/3 of the *c* values are lower than 0. At the weekly scale, the center of the distribution moves left with ~~the~~ a mean value of 0.43 ± 0.24. Half of the *c* values are lower than 0. At the monthly scale, the mean value is −0.04 ± 0.23, and 58% of the *c* values are lower than 0. At the annual scale, the mean value decreases to −0.37 ± 0.25, and 63% of the *c* values are lower than 0. These results support our conclusion that $1/b$ and *c* decrease as the time scale increases. Generally, the distribution of $1/b$ and *c* also moves left within each ecosystem type according to Figures 5 and 6.

The reduction ~~of~~ in $1/b$ and *c* indicates that the curves of the complementary functions move upwards as the time scale increases. Under non-humid conditions, the sigmoid function is a concave function, which means:

$$\frac{1}{2}[f(x_1) + f(x_2)] > f(\frac{x_1 + x_2}{2}) \qquad (8)$$

where, *f* is the concave function, and x_1 and x_2 represent any two values on the x-axis. Since most of the results follow the fitted line, the averaged results of the longer timestep will ~~go~~ move upwards in the two-dimensional space of E_{rad}/E_{pen}-E/E_{pen}, ~~so does~~as well the new fitted curve. Although under ~~the~~ super humid conditions, the SGC function is a convex function, there ~~is~~ are fewer data ~~in~~ under this condition as the time scale increases, and the shape of this part is almost unchanged (Figure 4a). ~~As f~~For the PGC function, when *x* is in the range of 0 to $1/\alpha$, most part of it is a concave function. For example, in the situation ~~that~~ where *c* is equal to 0, the second derivative is higher than 0 as long as *x* is lower than 2/3.

Furthermore, we found that the two key parameters~~,~~ *b* and *c* present a significant correlation, which provides additional evidence that ~~indicating~~ the two functions can substitute each other in a sense. In other words, the two functions with calibrated parameters substantially provide similar descriptions of the distribution of the results in the state space ($x = E_{rad}/E_{pen}$, $y = E/E_{pen}$). They can covert to each other in most situations since the two functions are generally equivalent to the linear asymmetric function when *x* is neither excessively large nor excessively small. The relationship can be described as follows: $1/b = 0.01c^2 + 0.11c + 0.24$ with R^2 being higher than 0.96 at the monthly scale (Figure ~~5~~7). The relationship remains~~keeps~~ at other time scales with a slight difference in the regression coefficients. At the daily scale, when *c* is equal to 0, the corresponding *b* is equal to 4.5, which is the same as that of the theoretical derivation in Brutsaert (2015).

In this study, the physical meaning of the Priestley-Taylor coefficient α, which represents the ratio of E_{PT} (the Priestley-Taylor evaporation) and E_{rad} with the default value of 1.26 (Priestley & Taylor, 1972; Brutsaert & Stricker, 1979), was retained. This fundamental definition of α may result in a smaller range of E_{rad}/E_{pen} in the PGC function. Liu et al. (2016) suggested that α_e (the calibrated α with $c = 0$) in the PGC function is only a weak analog of the Priestley-Taylor coefficient, and Brutsaert (2019) directly considered α_e as an adjustable parameter, which can be equal to or smaller than 1. We added the analysis that *c* is fixed to 0 and α is calibrated as α_e. This analysis showed that the two methods provide similar results (mean RMSE = 14.99 W m^{-2} for α_e vs 16.67 W m^{-2} for α), and the conclusion of the time scale issue is consistent by adopting either α or α_e in the analysis. The optimal α_e has a significantly negative linear relationship with the optimal c and the Pearson correlation coefficient is −0.8. This scenario suggests that calibrating either of the two parameters (α_e and c) is equivalent (Han et al., 2012).

3.5 Uncertainty analysis

3.5.1 Influence of ecosystem types

The evaluation merits of the generalized complementary functions may differ among ecosystem types. However, our results show that such variation generally does not affect our conclusion that the complementary functions perform best at the monthly scale. We show the performance of the two functions at multiple timescales for each ecosystem type in Table S3~~2~~. Generally, the SGC function and the PGC function perform best at the monthly scale in most ecosystem types (9 of 11) with the highest NSE and R^2, which is consistent with the overall results. The exceptions include a closed shrubland site (CSH, N = 1) and evergreen broadleaf forests (EBF, N = 8), in which the complementary functions do not perform ~~not~~ as well as in other ecosystem types. The CSH site (IT-Noe) has the highest NSE_H (0.11) and NSE_B (0.12) at the annual scale. In the EBF group, the highest NSE_H (0.15) and NSE_B (0.03) occur at the weekly scale, but the R^2 values at the weekly scale (R^2_H = 0.64; R^2_B= 0.62) and those at the monthly scale (R^2_H = 0.62; R^2_B = 0.61) are similar ~~close~~. The RMSEs at the weekly scale are 14.95 W m^{-2} and 16.08 W m^{-2} for the sigmoid function and polynomial function, respectively, and those values at the monthly scale are 12.36 W m^{-2} ($RMSE_H$) and 12.93 W m^{-2} ($RMSE_B$). We inferred that the abnormal results of these two exceptions are related to the lower NSE values in these ecosystem types. The mean NSE values at multiple time scales of CSH (−0.75) and EBF (−0.66) are negative, while the values of the other ecosystem types are all positive.

3.5.2 Performance at the seasonal scale

In consideration of the substantial discrepancy between the monthly results and the annual results, we added an analysis at the seasonal scale, which is between the two timesteps. The relationship between the estimated E_{est} (site mean values) and the observed E of the 88 sites at the seasonal scale is shown in Figure S1. For the SGC function, the regression result at the seasonal scale is similar to that at the monthly scale (Figure S1a and Figure 1c). The values of NSE_H (0.33), R^2_H (0.61), and $RMSE_H$ (10.16 W m^{-2}) at the seasonal scale are between the monthly results and the yearly results (Table 1). For the PGC functions, the regression result at the seasonal scale is extremely close to that at the yearly scale (Figure S1b and Figure 3d). The evaluation merits (NSE_B = 0.31; R^2_B = 0.63; $RMSE_B$ = 9.94 W m^{-2}) also range between the monthly results and the yearly results (Table 1). These results indicate that the decline ~~of~~ in ~~the~~ model efficiency has already occurred at the seasonal scale and support our conclusion that the complementary functions perform best at the monthly scale.

In addition, ~~3.5.3 Influence of energy balance residual correction methods~~

~~So far, there are mainly two methods for surface energy closure correction in the complementary studies. In the first method, the residual term is attributed into latent heat directly as the "energy residual" (ER) closure correction (e.g., Ershadi et al., 2014; Han and Tian 2018), which is adopted in above analysis. The second method is called the "Bowen~~

~~ratio" (BR) closure correction, in which the residual term is attributed into sensible heat and latent heat by preserving Bowen ratio (e.g., Twine et al., 2000; Ma et al., 2015a). Based on different correction methods, the evaluation results of the model performance may differ. Thus, we recalculated our results by adopting the BR energy closure correction method. We found the mean value of 1/*b* changes from 0.29 ± 0.04 (ER) to 0.40 ± 0.05 (BR) and the mean value of *c* changes from −0.04 ± 0.23 (ER) to 0.63 ± 0.24 (BR) at monthly scale. It indicates the key parameters could be affected by adopting different correction methods. However, the results based on the BR method also support that the complementary functions perform best on evaporation estimation at monthly scale (Table 2). The NSE and R^2 vales increase from daily scale to monthly scale, and decrease from monthly scale to yearly scale, just following the pattern showed in Table 1. Generally, the evaluation results based on the BR method are worse than those based on the ER method. For example, when the ER method was replaced by the BR method the NSE and R^2 values decrease ($\Delta NSE_H = -0.15$; $\Delta NSE_B = -0.23$; $\Delta R^2_H = -0.07$; $\Delta R^2_B = -0.07$) and the RMSE values increase ($\Delta RMSE_H = 1.36$ W m^{-2}; $\Delta RMSE_B = 1.56$ W m^{-2}) at monthly scale. Ershadi et al. (2014) also found that the modeled E_{est} values by the PM equation, the AA approach and the modified Priestley-Taylor model (PT-JPL) show higher agreement with the ER corrected evaporation instead of the BR corrected evaporation. Ershadi et al. (2014) inferred the reason is that the observed sensible heat flux is more reliable than the observed latent heat flux. The measurement of latent heat by the EC tower may be confounded by minor instabilities when the boundary layer shrinks at night. To summarize, although the different energy closure correction methods have some influences on the key parameters and model efficiencies, they do not affect our conclusion that the~~

~~generalized complementary functions perform best at monthly scale.~~ we also tested the influence of the different energy balance closure methods. The results based on both the “energy residual” (ER) closure correction (e.g., Ershadi et al., 2014; Han and Tian 2018) and the “Bowen ratio” (BR) closure correction support our conclusion that the generalized complementary functions perform best at the monthly scale (Table S4).

4. Conclusions

In this study, evaporation estimations were~~as~~ assessed ~~over~~ at 88 EC monitoring sites at multiple time scales (daily, weekly, monthly, and yearly) by using two generalized complementary functions (the SGC function and the PGC function). The performances of the complementary functions at multiple time scales were~~as~~ compared, and the variation ~~of~~ in the key parameters at different time scales was explored. The main findings are summarized as follows:

(1) The sigmoid and polynomial generalized complementary functions exhibit higher~~the highest~~ skill in estimating evaporation~~ estimation~~ at the monthly scale than at the other evaluated scales. The highest evaluation merits were obtained at this time scale. The accuracy of the complementary functions highly depends on the calculation timestep. The NSE increases from the daily scale (0.26, averaged by NSE_H and NSE_B) to the weekly scale (0.37) and monthly scale (0.53), while it decreases at the seasonal scale (0.32) and the annual scale (0.22). The regression parameters between estimated E_{est} and observed site mean E also support this conclusion for the PGC function. The variations among the different ecosystem

types or between different energy balance closure methods~~energy balance correction methods~~ generally have no effect on this conclusion. Further evaporation estimation studies with~~by using the~~ complementary functions can choose the monthly timestep to achieve the most accurate results.

(2) The SGC function and the PGC function are approximately identical under non-humid environments, while the SGC function performs better under super humid conditions implied by high values of x (> $1/\alpha$) when the PGC function is theoretically useless ($E_{est} > E_{pen}$). At daily and weekly time scales, a substantial number of~~quite a few~~ ecosystems can experience frequent high x values,~~occurrences~~ and thus, the SGC function performs slightly better than the PGC function at these time scales. However, both functions~~they~~ perform very similarly at monthly and annual time scales ~~as~~ with few high x ~~occurrences~~values. In addition~~Besides~~, the performance of the PGC function is more sensitive to the timestep than that of the SGC function.

(3) The key parameter b of the SGC function increases and the key parameter c of the PGC function decreases~~d~~ as the time scale increases. The value of $1/b$ is a quadratic function of c with a higher R^2 (> 0.96). The relationship at the monthly scale can be described as~~:~~ $1/b = 0.01c^2 + 0.11c + 0.24$. This relationship~~It~~ indicates that the two functions serve as ~~can~~ substitutes~~ each other~~ to some extent.

In this study, i~~n order~~ to ~~find~~ determine the most suitable time scale for applying the complementary principle, the key parameters (*b* and *c*) were calibrated to achieve the best model performance at each timescale. Further studies on the prognostic application of the complementary principle could focus on the reasonable prediction of the key parameters, and with the predictable flexible parameters at different timescales, the complementary principle could be integrated into hydrological models to reduce the uncertainty associated with evaporation estimations.

Code/Data availability

All the data used in this study are from FLUXNET (http://fluxnet.fluxdata.org). The intermediate data are available on request from the corresponding author (tianfq@mail.tsinghua.edu.cn).

Author contribution

Songjun Han and Fuqiang Tian designed the experiments and Liming Wang carried them out. Liming Wang developed the model code and performed the simulations. Liming Wang prepared the manuscript with contributions from all co-authors.

Competing interests

The authors declare that they have no conflict of interest.

Acknowledgements

We are grateful for the financial support from National Science Foundation of China (NSFC

51825902, 51579249). We thank the scientists of FLUXNET (http://fluxnet.fluxdata.org) for their generous sharing of their eddy flux data. We are grateful to the reviewers and the editors who provided valuable comments and suggestions for this work.

References

Allen, R. G., Pereira, L. S., Raes, D., Smith, M.: Crop evapotranspiration: Guidelines for computing crop water requirements. FAO irrigation and drainage paper No. 56, Food and Agricultural Organization of the U.N., Rome, Italy, 1998.

Baldocchi, D., Falge, E., Gu, L., Olson, R., Hollinger, D., Running, S. et al.: FLUXNET: A new tool to study the temporal and spatial variability of ecosystem-scale carbon dioxide, water vapor, and energy flux densities. Bull Amer. Meteor. Soc., 82(11), 2415–2434, 2001. https://doi.org/10.1175/1520-0477(2001)082<2415:FANTTS>2.3.CO;2

Bouchet, R. J.: Evapotranspiration réelle et potentielle, signification climatique. IAHS Publ, 62, 134-142, 1963.

Brubaker, K. L., Entekhabi, D.: Analysis of feedback mechanisms in land-atmosphere interaction. Water Resour. Res., 32(5), 1343-1357, 1996. https://doi.org/10.1029/96wr00005

Brutsaert, W.: A generalized complementary principle with physical constraints for land-surface evaporation. Water Resour. Res., 51(10), 8087-8093, 2015. https://doi.org/10.1002/2015wr017720

Brutsaert, W.: Spatial distribution of global landscape evaporation in the early twenty first century by means of a generalized complementary approach. J. Hydrometeorol., 21(2), 287-298, 2019. https://doi.org/ 10.1175/JHM-D-19-0208.1

Brutsaert, W., Li, W., Takahashi, A., Hiyama, T., Zhang, L., Liu, W. Z.: Nonlinear advection-aridity method for landscape evaporation and its application during the growing season in the southern Loess Plateau of the Yellow River basin. Water Resour. Res., 53(1), 270-282, 2017. https://doi.org/ 10.1002/2016wr019472

Brutsaert, W., Parlange, M. B.: Hydrologic cycle explains the evaporation paradox. Nature, 396(6706), 30-30, 1998. https://doi.org/ 10.1038/23845

Brutsaert, W., Stricker, H.: Advection-Aridity approach to estimate actual regional evapotranspiration. Water Resour. Res., 15(2), 443-450, 1979. https://doi.org/ 10.1029/WR015i002p00443

Budyko, M.I.: Climate and life (Vol. 508). New York: Academic press, 1974.

Crago, R., Crowley, R.: Complementary relationships for near-instantaneous evaporation. J. Hydrol., 300(1-4), 199-211. https://doi.org/10.1016/j.jhydrol.2004.06.002, 2005.

Crago, R. D., Qualls, R. J.: Evaluation of the generalized and rescaled complementary evaporation relationships. Water Resour. Res., 54(10), 8086-8102, 2018. https://doi.org/10.1029/2018wr023401

Ershadi, A., McCabe, M. F., Evans, J. P., Chaney, N. W., Wood, E. F.: Multi-site evaluation of terrestrial evaporation models using FLUXNET data. Agric. For. Meteorol., 187, 46–61, 2014. https://doi.org/10.1016/j.agrformet. 2013.11.008

Fu, B. P.: On the calculation of the evaporation from land surface (in Chinese), Sci. Atmos. Sin., 5(1), 23 – 31, 1981.

Han, S. J., Hu, H. P., Tian, F. Q.: A nonlinear function approach for the normalized complementary relationship evaporation model. Hydrol. Processes, 26(26), 3973-3981, 2012. https://doi.org/10.1002/hyp.8414

Han, S. J, Hu, H. P., Tian, F. Q.: Evaluating the Advection-Aridity model of evaporation using data from field-sized surfaces of HEIFE. IAHS Publ., 322(2):9-14, 2008.

Han, S. J., Hu, H. P., Yang, D. W., Tian, F. Q.: A complementary relationship evaporation model referring to the Granger model and the advection-aridity model. Hydrol. Processes, 25(13), 2094-2101, 2011. https://doi.org/10.1002/hyp.7960

Han, S. J., Tian, F. Q.: Derivation of a sigmoid generalized complementary function for evaporation with physical constraints. Water Resour. Res., 54(7), 5050-5068, 2018.

https://doi.org/10.1029/2017wr021755

Han, S., Tian, F.: Complementary principle of evaporation: From original linear relationship to generalized nonlinear functions. Hydrol. Earth Syst. Sci., 24(5), 2269-2285, 2020. https://doi.org/10.5194/hess-24-2269-2020

Hobbins, M. T., Ramirez, J. A., Brown, T. C.: The complementary relationship in estimation of regional evapotranspiration: An enhanced Advection-Aridity model. Water Resour. Res., 37(5), 1389-1403, 2001. https://doi.org/10.1029/2000wr900359

Hobbins, M. T., Ramirez, J. A.: Trends in pan evaporation and actual evapotranspiration across the conterminous U.S.: Paradoxical or complementary? Geophys. Res. Lett. 31.13:405-407, 2004. https://doi.org/10.1029/2004GL019846

Hu, Z. Y., Wang, G. X., Sun, X. Y., Zhu, M. Z., Song, C. L., Huang, K. W., Chen, X. P.: Spatial-temporal patterns of evapotranspiration along an elevation gradient on Mount Gongga, Southwest China. Water Resour. Res., 54(6), 4180-4192, 2018. https://doi.org/10.1029/2018wr022645

Kahler, D. M., Brutsaert, W.: Complementary relationship between daily evaporation in the environment and pan evaporation. Water Resour. Res, 42(5), 2006. https://doi.org/10.1029/2005WR004541

Legates D. R., Mccabe G. J.: Evaluating the use of “goodness-of-fit” Measures in hydrologic and hydroclimatic model validation. Water Resour. Res., 35(1):233-241, 1999. https://doi.org/10.1029/1998wr900018

Liu, X. M., Liu, C. M., Brutsaert, W.: Regional evaporation estimates in the eastern monsoon region of China: Assessment of a nonlinear formulation of the complementary principle. Water Resour. Res., 52(12), 9511-9521, 2016. https://doi.org/10.1002/2016wr019340

Ma, N., Szilagyi, J., Zhang, Y., Liu, W.: Complementary relationship-based modeling of terrestrial evapotranspiration across China during 1982–2012: Validations and spatiotemporal analyses. J. Geophys. Res. Atmos., 124, 4326–4351, 2019. https://doi.org/10.1029/2018JD029850

Ma, N., Zhang, Y. S., Szilagyi, J., Guo, Y. H., Zhai, J. Q., Gao, H. F.: Evaluating the complementary relationship of evapotranspiration in the alpine steppe of the Tibetan Plateau. Water Resour. Res., 51(2), 1069-1083, 2015a. https://doi.org/10.1002/2014wr015493

Ma, N., Zhang, Y. S., Xu, C. Y., Szilagyi, J.: Modeling actual evapotranspiration with routine meteorological variables in the data-scarce region of the Tibetan Plateau: Comparisons and implications. J. Geophys. Res. Biogeosci., 120(8), 1638-1657, 2015b. https://doi.org/10.1002/2015jg003006

Monin, A., Obukhov, A.: Basic laws of turbulent mixing in the surface layer of the atmosphere. Contrib. Geophys. Inst. Acad. Sci. USSR, 151(163), e187, 1954.

Monteith, J. L.: Evaporation and environment (pp. 205-234): Paper presented at the Symposia of the society for experimental biology. Cambridge University Press (CUP) Cambridge, 1965.

Morton, F. I.: Operational estimates of areal evapo-transpiration and their significance to the science and practice of hydrology. J. Hydrol., 66(1-4), 1-76, 1983. https://doi.org/10.1016/0022-1694(83)90177-4

Neelin, J. D., Held, I. M., Cook, K. H.: Evaporation-wind feedback and low-frequency variability in the tropical atmosphere. J. Atmos. Sci., 44(16), 2341-2348, 1987. https://doi.org/ 10.1175/1520-0469(1987)044<2341:Ewfalf>2.0.Co;2

Parlange, M. B., Katul, G. G.: An advection-aridity evaporation model, Water Resour. Res., 28, 127-132, 1992. https://doi.org/10.1029/91WR02482

Penman, H. L.: The dependence of transpiration on weather and soil conditions. J. Soil Sci., 1(1), 74-89, 1950. https://doi.org/10.1111/j.1365-2389.1950.tb00720.x

Penman, H. L.: Natural evaporation from open water, bare soil and grass. Proc. R. Soc. London, Ser. A., 193(1032), 120-145, 1948. https://doi.org/10.1098/rspa.1948.0037

Priestley, C. H. B., Taylor, R. J.: On the assessment of surface heat-flux and evaporation using large-scale parameters. Mon. Weather Rev., 100(2), 81-92, 1972. https://doi.org/10.1175/1520-0493(1972)100<0081:Otaosh>2.3.Co;2

Qualls, R. J., Gultekin, H.: Influence of components of the advection-aridity approach on evapotranspiration estimation. J. Hydrol., 199(1-2), 3-12, 1997. https://doi.org/10.1016/S0022-1694(96)03314-8

Shukla, J., Mintz, Y.: Influence of land-surface evapo-transpiration on the earths climate. Science, 215(4539), 1498-1501, 1982. https://doi.org/10.1126/science.215.4539.1498

Sugita, M., Usui, J., Tamagawa, I., & Kaihotsu, I.: Complementary relationship with a convective boundary layer model to estimate regional evaporation. Water Resources Research, 37(2), 353-365, 2001. https://doi.org/10.1029/2000wr900299

Szilagyi, J.: On the inherent asymmetric nature of the complementary relationship of evaporation. Geophysical Research Letters, 34(2), L02405, 1-6, 2007. https://doi.org/10.1029/2006gl028708

Twine, T. E., Kustas, W. P., Norman, J. M., Cook, D. R., Houser, P., Meyers, T. P., Wesely, M. L.: Correcting eddy-covariance flux underestimates over a grassland. Agric. For. Meteorol., 103(3), 279-300, 2000. https://doi.org/10.1016/S0168-1923(00)00123-4

Wang, K. C., Dickinson, R. E.: A review of global terrestrial evapotranspiration: observation, modeling, climatology, and climatic variability. Rev. Geophys., 50, 2012. https://doi.org/10.1029/2011rg000373

Wang, L.M., Tian, F. Q., Han, S. J., Wei, Z. W.: Determinants of the asymmetric parameter in the generalized complementary principle of evaporation. Water Resour. Res, 2020, 56, e2019WR026570 ~~(accepted)~~. https://doi.org/10.1029/2019WR026570

Zhang, L., Cheng, L., Brutsaert, W.: Estimation of land surface evaporation using a generalized nonlinear complementary relationship. J. Geophys. Res. Atmos., 122(3), 1475-1487, 2017. https://doi.org/10.1002/2016jd025936

Zhou, H., Han, S., Liu, W.: Evaluation of two generalized complementary functions for annual evaporation estimation on the loess plateau, china. J. Hydrol., 587, 124980, 2020. https://doi.org/10.1016/j.jhydrol.2020.124980

List of Figure Captions

Figure 1. The estimated evaporation based on the SGC function (equation (1)) vs the observed site mean evaporation at the daily scale (a), weekly scale (b), monthly scale (c) and yearly scale (d). Each dot represents the site mean result (N = 88 in each panel). The regression equations and determination coefficients (R^2) were calculated by the site mean results of the 88 EC sites.

Figure 2. Plots of E/E_{pen} with respect to $E_{\mathrm{rad}}/E_{\mathrm{pen}}$ for five selected sites at multiple time scales. The black dots represent the observations; the red lines represent the SGC function; the green lines represent the PGC function; the blue lines are the P-T and Penman boundary lines. ENF, evergreen needleleaf forests; DBF, deciduous broadleaf forests; WSA, woody savannas; CRO, croplands; GRA, grasslands.

Figure 3. As in Figure 1 except for PGC function (equation (5)).

Figure 4. Plots of the SGC equation (1) with $\alpha = 1.26$ and varying $1/b$ values at multiple time scales (a). Plots of the PGC equation (5) with $\alpha = 1.26$ and varying c values at multiple time scales (b). The blue lines are the P-T and Penman boundary lines.

Figure 5. Distribution of the key parameter $1/b$ at daily scale (a), weekly scale (b), monthly scale (c) and yearly scale (d): EBF, evergreen broadleaf forests (8); ENF, evergreen needleleaf forests (27); DBF, deciduous broadleaf forests (13); MF, mixed forests (5); Shrub (12), closed shrubland, open shrublands, woody savannas and savannas; CRO, croplands (6); WET, permanent wetlands (2).

Figure 6. Distribution of the key parameter c at daily scale (a), weekly scale (b), monthly scale (c) and yearly scale (d): EBF, evergreen broadleaf forests (8); ENF, evergreen

needleleaf forests (27); DBF, deciduous broadleaf forests (13); MF, mixed forests (5); Shrub (12), closed shrubland, open shrublands, woody savannas and savannas; CRO, croplands (6); WET, permanent wetlands (2).

Figure 7. Relationships between 1/*b* and *c* at the monthly scale.

Table 1. The evaluation merits (NSE, R^2 and RMSE in W m^{-2}) of the two generalized complementary functions using the "energy residual" (ER) closure correction method. The subscript H and B correspond to the SGC function proposed in Han and Tian (2018) and the PGC function proposed in Brutsaert (2015), respectively.

	Day	Week	Month	Season	Year
NSE_H	0.33	0.44	0.55	0.33	0.18
NSE_B	0.19	0.3	0.50	0.31	0.25
R^2_H	0.62	0.7	0.74	0.61	0.61
R^2_B	0.61	0.7	0.75	0.63	0.63
$RMSE_H$	24.56	17.67	13.20	10.16	7.33
$RMSE_B$	26.83	19.17	13.70	9.94	6.96

~~**Table 2.** The evaluation merits (NSE, R^2 and RMSE in W m^{-2}) of the two generalized complementary functions using the "Bowen ratio" (BR) closure correction method. The subscript H and B correspond to the SGC function proposed in Han & Tian (2018) and the PGC function proposed in Brutsaert (2015), respectively.~~

~~—~~	~~Day~~	~~Week~~	~~Month~~	~~Season~~	~~Year~~
~~NSE_H~~	~~0.01~~	~~0.23~~	~~0.4~~	~~0.17~~	~~−0.07~~
~~NSE_B~~	~~−0.28~~	~~0.03~~	~~0.27~~	~~0.11~~	~~−0.23~~
~~R^2_H~~	~~0.53~~	~~0.62~~	~~0.67~~	~~0.54~~	~~0.52~~
~~R^2_B~~	~~0.52~~	~~0.61~~	~~0.68~~	~~0.55~~	~~0.52~~
~~$RMSE_H$~~	~~26.62~~	~~18.9~~	~~14.56~~	~~11.3~~	~~7.88~~
~~$RMSE_B$~~	~~29.77~~	~~20.59~~	~~15.26~~	~~11.3~~	~~8.03~~

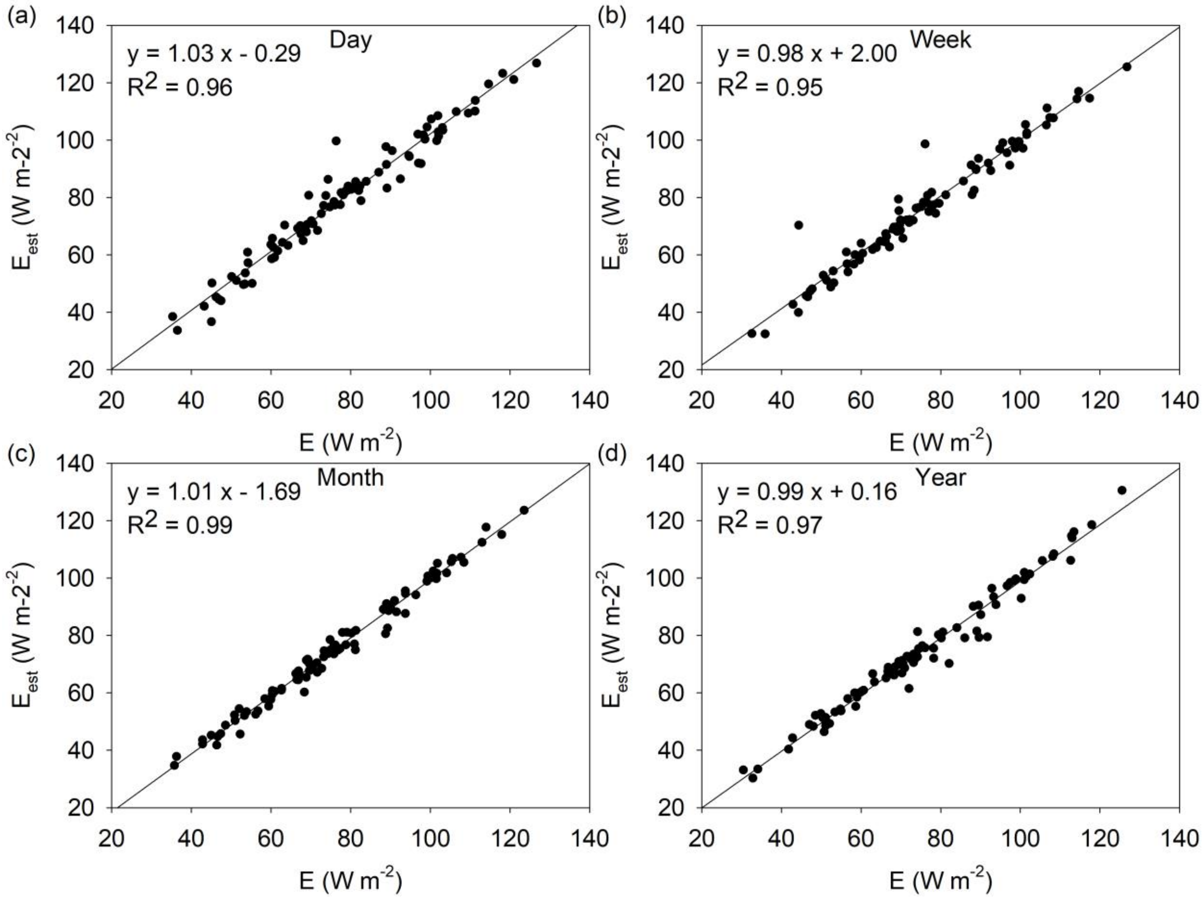

Figure 1. The estimated evaporation based on the SGC function (equation (1)) vs the observed site mean evaporation at the daily scale (a), weekly scale (b), monthly scale (c) and yearly scale (d). Each dot represents the site mean result (N = 88 in each panel). The regression equations and determination coefficients (R^2) were calculated by the site mean results of the 88 EC sites.

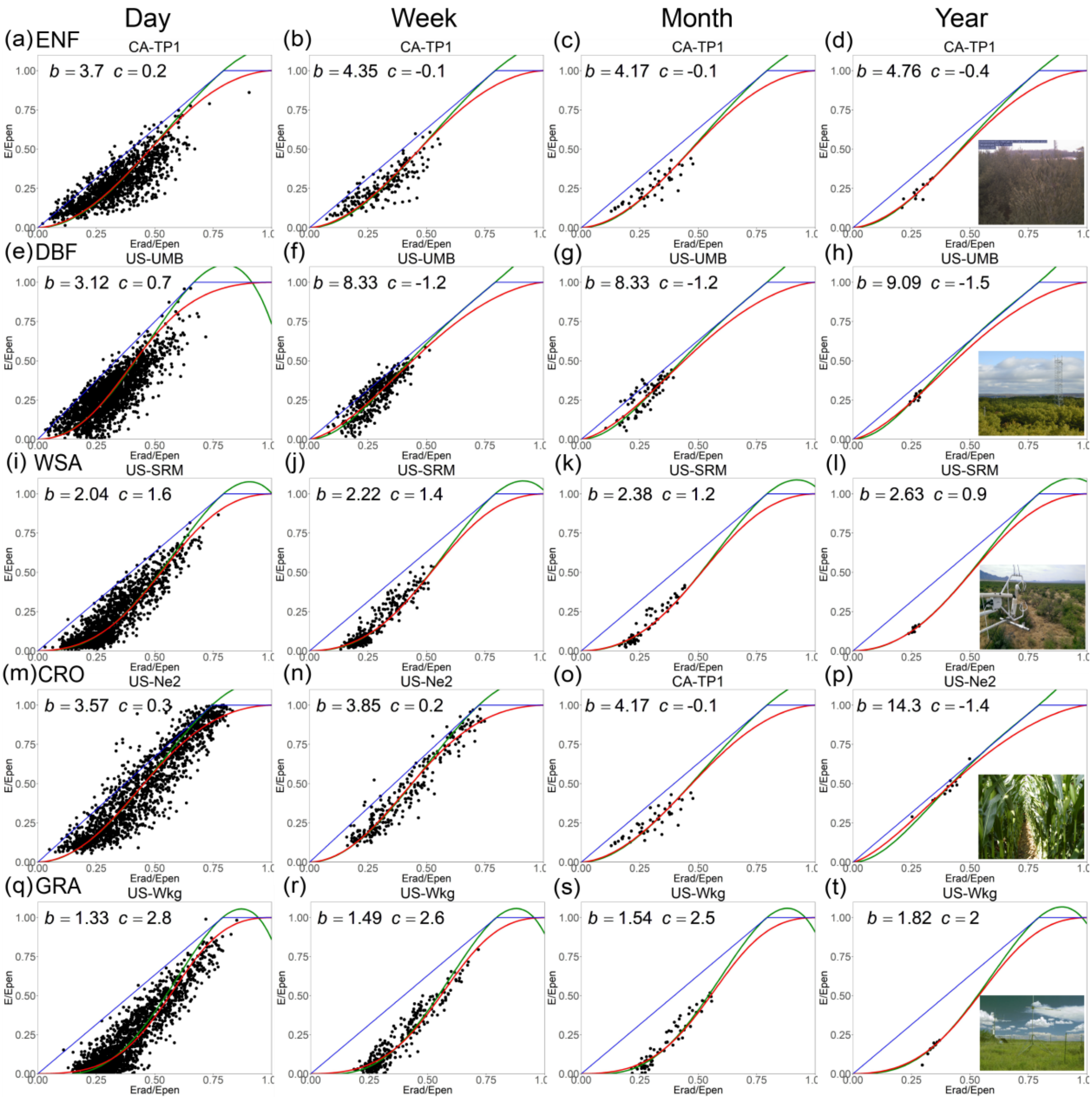

Figure 2. Plots of E/E_{pen} with respect to $E_{\mathrm{rad}}/E_{\mathrm{pen}}$ for five selected sites at multiple time scales. The black dots represent the observations; the red lines represent the SGC function; the green lines represent the PGC function; the blue lines are the P-T and Penman boundary lines. ENF, evergreen needleleaf forests; DBF, deciduous broadleaf forests; WSA, woody savannas; CRO, croplands; GRA, grasslands.

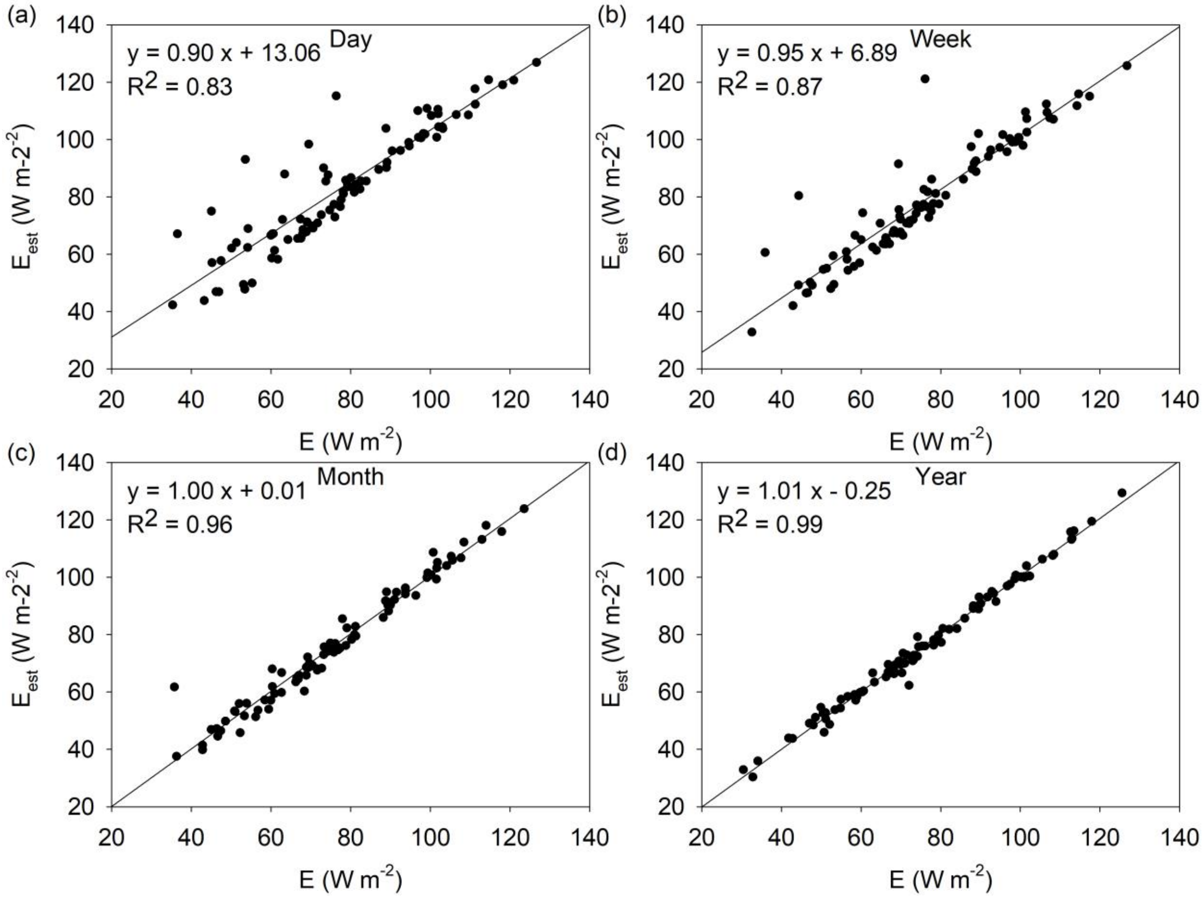

Figure 3. As in Figure 1 except for PGC function (equation (5)).

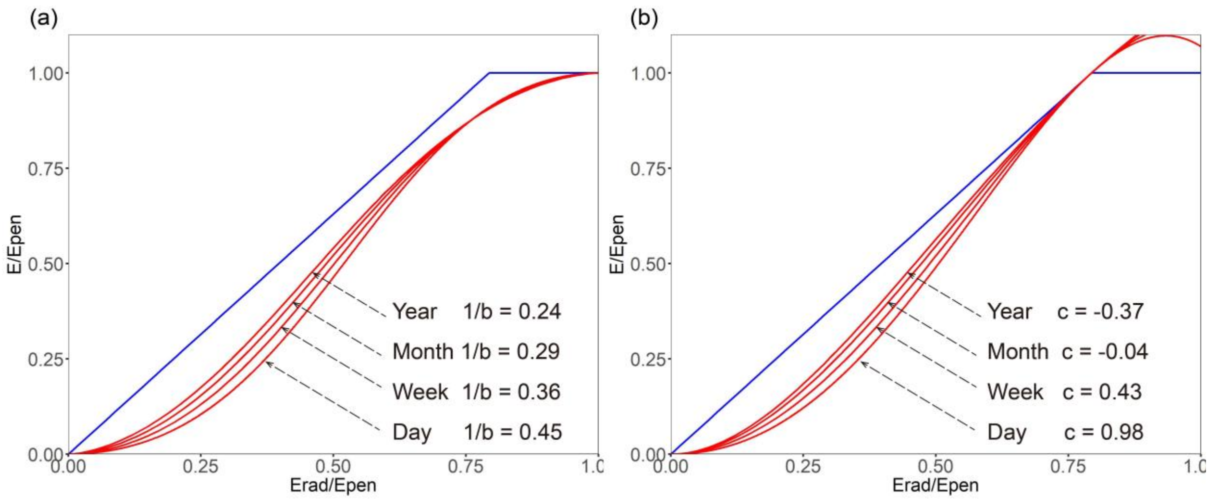

Figure 4. Plots of the SGC equation (1) with $\alpha = 1.26$ and varying $1/b$ values at multiple time scales (a). Plots of the PGC equation (5) with $\alpha = 1.26$ and varying c values at multiple time scales (b). The blue lines are the P-T and Penman boundary lines.

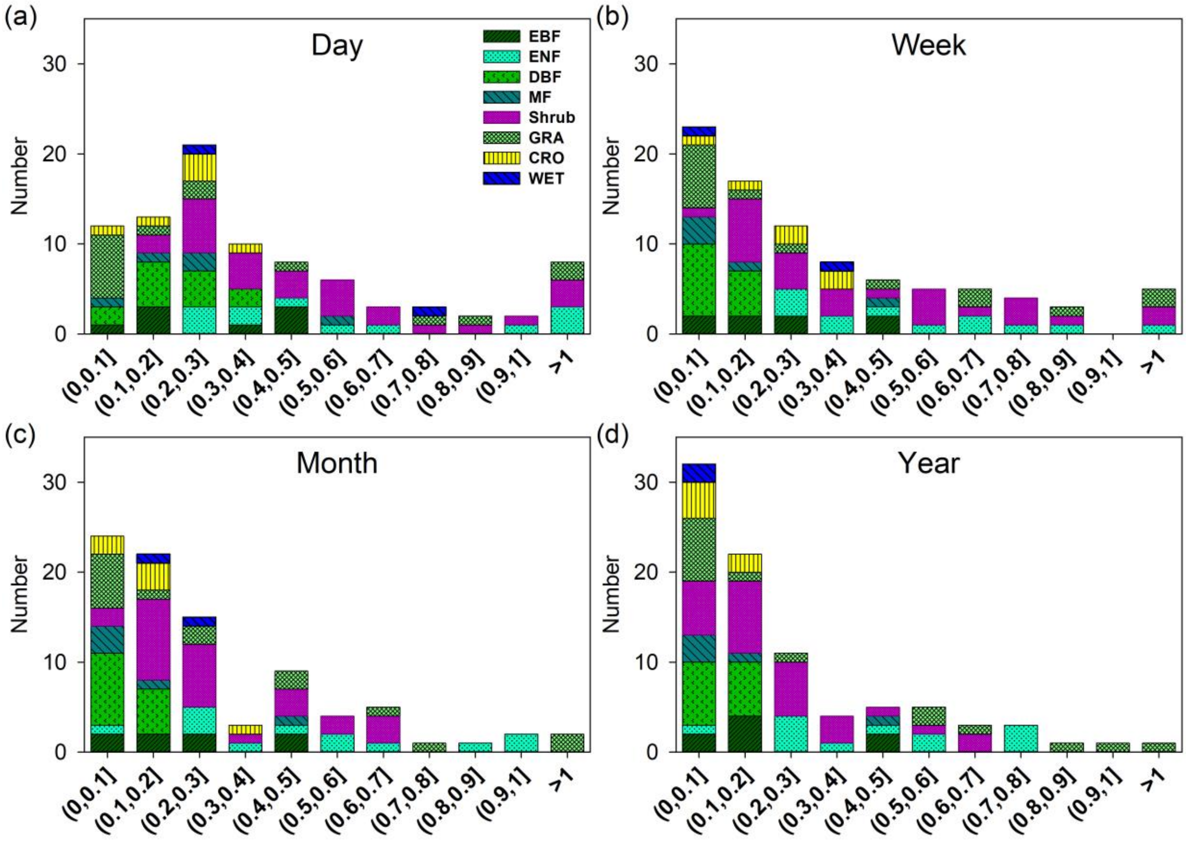

Figure 5. Distribution of the key parameter $1/b$ at daily scale (a), weekly scale (b), monthly scale (c) and yearly scale (d): EBF, evergreen broadleaf forests (8); ENF, evergreen needleleaf forests (27); DBF, deciduous broadleaf forests (13); MF, mixed forests (5); Shrub (12), closed shrubland, open shrublands, woody savannas and savannas; CRO, croplands (6); WET, permanent wetlands (2).

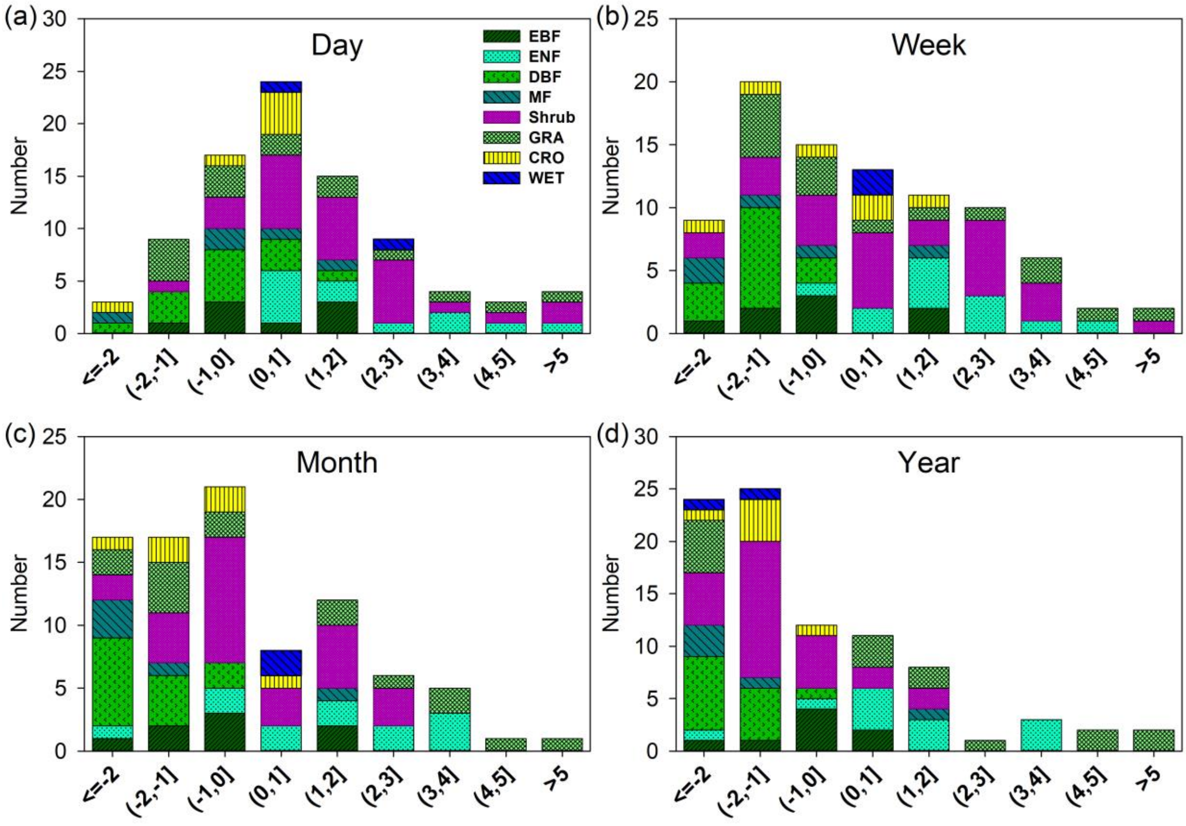

Figure 6. Distribution of the key parameter *c* at daily scale (a), weekly scale (b), monthly scale (c) and yearly scale (d): EBF, evergreen broadleaf forests (8); ENF, evergreen needleleaf forests (27); DBF, deciduous broadleaf forests (13); MF, mixed forests (5); Shrub (12), closed shrubland, open shrublands, woody savannas and savannas; CRO, croplands (6); WET, permanent wetlands (2).

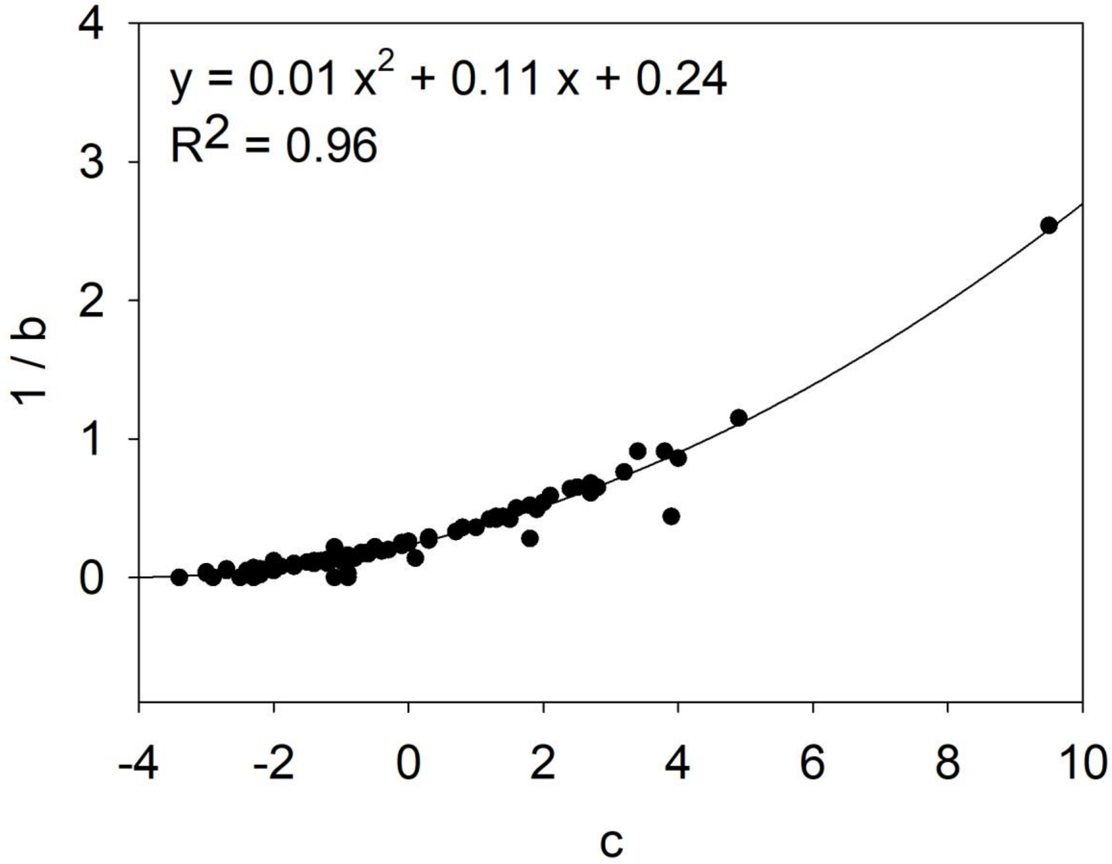

Figure 7. Relationships between 1/*b* and *c* at the monthly scale.